Determining Fatigue through Real-Time Sweat Analysis

M.R. Thomas

Delft University of Technology

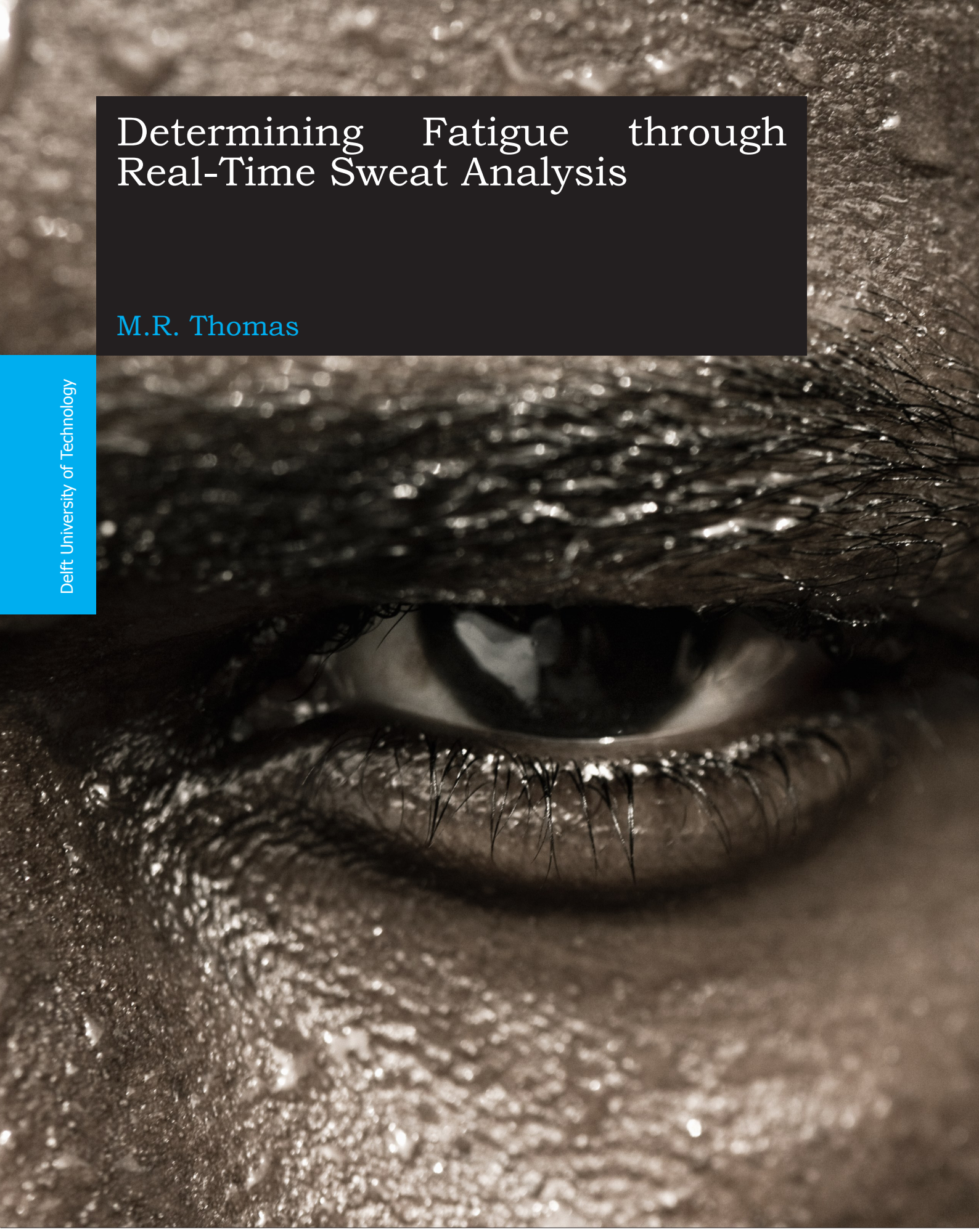

TU Delft Delft University of Technology

Challenge the future

Determining Fatigue through Real-Time Sweat Analysis

by

M.R. Thomas

in partial fulfillment of the requirements for the degree of

Master of Science

in Mechanical Engineering

at the Delft University of Technology,
to be defended publicly on Tuesday January 21, 2019 at 14:00

Student number: 4062922
Project duration: February 1, 2018 – January 21, 2019

Thesis committee:
Prof. dr. P.J. French — TU Delft, supervisor
Prof. dr. H.E.J. Veeger — TU Delft, supervisor
Prof. dr. A. Bossche — TU Delft
Dr. D.H. Plettenburg — TU Delft

TU Delft Delft University of Technology

Acknowledgment

This report represents the results of my graduation project, needed to receive my master's degree in Mechanical Engineering at the Delft University of Technology. Out of all the projects I have done during my years at the TU Delft, this has been the most interesting one. The aim of this research is to determine fatigue by designing a sweat analysis device which would be able to tell the user how tired they are. Firstly, I would like to thank Paddy French for introducing me to this project in the summer of 2017 when I was still struggling to find a thesis topic that I was really interested in. The moment I heard the proposal I was interested. I would also like to thank Andre Bossche, Jeroen Bastemeijer and Annemarijn Steilen for their input during our weekly meetings. Without your input, this project would have been more difficult. I would also like to thank Dirk-Jan Veeger who brought me into contact with Hein Daanen. The first few research papers and book that I received from Hein, were the foundation of my project and I also truly appreciated you volunteering to participate in my experiment. Also I would like to thank the PhD candidate of Hein, Lisa Klous, for helping me with carrying out the experiment in the climate room at the VU Amsterdam. Also a thanks to my friends Destry, Fabian, Naphur, Sergej, Patrick, Rinke and Timothy for your support and motivation especially in the times I was slacking off. Last but not least, my parents, Omaira and Michael, Xiomara, Zakir and the rest of my family in Curaçao and Suriname, thank you for being there for me during my highs and lows in life throughout the years since moving to Delft. I hope you enjoy reading my thesis as I have enjoyed this project. Masha danki!

M.R. Thomas
Delft, January 2019

Abstract

At present, commercially available wearable sensors are only capable of tracking an individual's physical activities and vital signs (such as heart rate). However, these devices fail to provide insight into fatigue itself. Fatigue is a broad term with many meanings. Fatigue in this paper refers to physiological changes where the muscle becomes fatigued due to increased lactate concentration during high physical activities. Real-time measurements of thermal sweat out of the eccrine glands could enable such insight because it contains physiologically and metabolically rich information that can be retrieved non-invasively. Thermal sweat that secretes out of the eccrine glands contains multiple inorganic constituents such as salt and potassium, nitrogen compounds such as ammonia and urea, and sugars such as glucose and lactate. Most literature agrees that ammonia is a potential constituent for determining the state of muscular fatigue. Different methods were proposed for real-time ammonia monitoring. Out of all these methods, a concept was designed using MOS sensors which measures ammonia concentration in a gas phase. This design was tested by letting participants perform an incremental cycling exercise up to the point while monitoring the ammonia concentration, temperature, humidity, and respiratory exchange ratio to validate whether the sensor is able to determine fatigue. The results are inconclusive whether it is able to determine fatigue through real-time ammonia monitoring.

Contents

1

Introduction

Recently, advances in information technology have made it possible to augment and improve the feedback athletes receive during training and competition. Moreover, modern technology has had such a profound impact on sport that many athletes and coaches now consider information derived from technology to be a valuable asset in performance increase [1].

Coaches strive constantly to improve the performance of athletes. The most important aspect of their role is to provide the athlete with a practice environment that is conducive to effective and efficient learning. One way of doing so is by continuously monitoring the athletes using wearable devices. Commercially available wearable devices, which in 2018 is a 5.8 billion dollar industry [2], enable near real-time continuous monitoring of individual's physical activities such as steps counter and physiological measures such as heart rate. These wearable sensor, also known as "smart-watches" has also interest in fatigue monitoring.

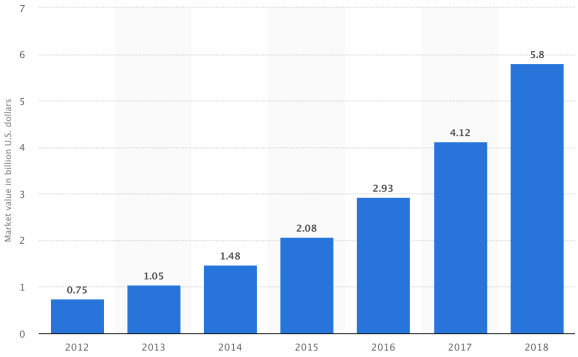

Figure 1.1: This statistic provides a forecast for the market value of the wearable device market from 2012 to 2018. The global market for wearable technology is forecast to grow to around six billion U.S. dollars by 2018 according to the source. As of the end of 2016, Fitbit held the largest market share of wearables worldwide, followed by Xiaomi and Apple.

However, all these devices fail to provide insight into fatigue itself. Measurement of human perspiration could enable such insight. Sweat constituents contains physiologically and metabolically rich information, which are connected to different physiological processes, that can be retrieved non-invasively [3] [4]. The ability to measure fatigue has many potential in endurance sports. Fatigue data can be used to optimize training or used during a competition as a strategy tool for example conserving energy during cycling or a marathon. This report will propose a method to determine fatigue through real-time sweat analysis.

In order to determine fatigue, fatigue itself must be defined. The term fatigue can be described as a

progressive phenomenon developed over time, resulting from a continuous physical or mental effort. In terms of classification, fatigue can be subdivided into the following subjective fatigue, objective fatigue and physiological fatigue. Within physiological changes which leads fatigue can be derived from several cerebral regions, the neuromuscular junction or the muscle fibres (Figure 1.2).

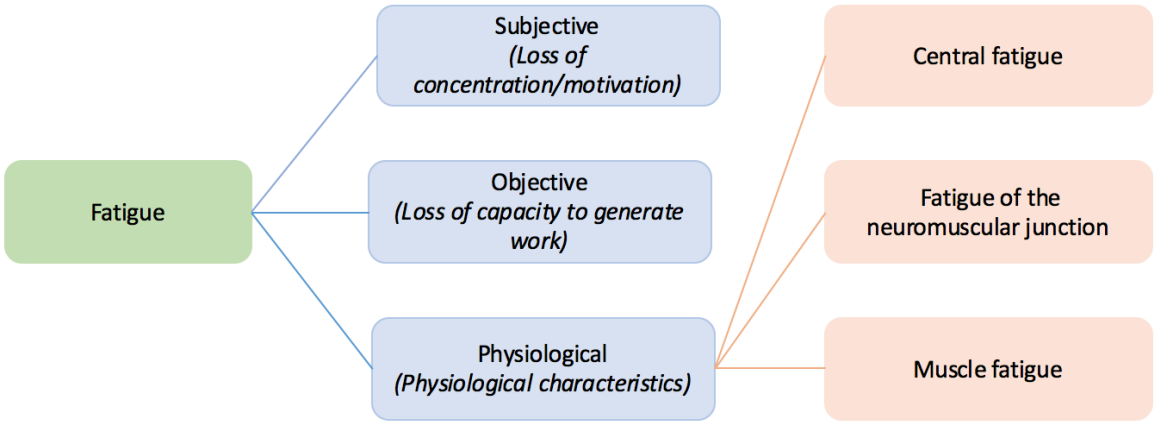

Figure 1.2: Classification of Fatigue State and Produced Effects [5] [6]

Fatigue in this paper is being characterized, from the muscular point of view, as the inability to maintain strength [7]. Under high intensity training, high energy consumption results in an imbalance between the glycolysis process and the aerobic consumption rate of pyruvic acid in order to break pyruvic acid into CO_2 and H_2O (Figure 1.3). This imbalance will lead to an anaerobic process which converts pyruvate into lactate, which is the burning sensation you feel also known as muscle acidification. This an important factor that leads to the inability to further perform a task or sustain an effort, or to the inability to reach the same initial level of maximal voluntary contraction (MVC) force [8] [9].

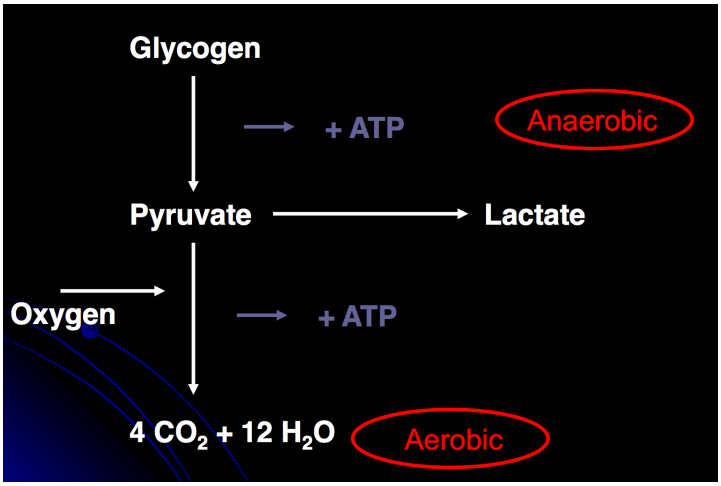

Figure 1.3: Aerobic and anaerobic energy production

2

Sweat Composition

Sweating can be classified in two groups: the thermal sweat, through eccrine glands, and the mental or emotional sweating, though apocrine glands [10]. Eccrine glands (Figure 2.1) cover almost the entire body, with the exception of the palms and soles. They have a tubular structure with a deep sub-dermal coiled secretory section which is connected to a duct which passes through the skin. The primary function of eccrine sweat glands is thermoregulation [11]. Apocrine glands (Figure 2.2) are the largest and occur in the axillae, areola of nipple and genital areas and they produce a viscous sweat containing lipids, cholesterol and steroids [11]. This paper will analyze thermal sweat out of the eccrine glands. This chapter is mostly based of the book "Physiology of human perspiration" written by Dr. Y. Kuno (1934) [10]

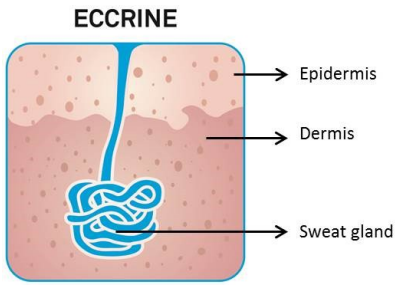

Figure 2.1: Eccrine sweat glands

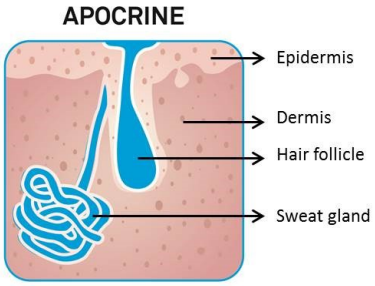

Figure 2.2: Apocrine sweat glands

2.1. Chemicals of Sweat

The sweat contains manifold constituents, but all of them are so small in amount that the total solid component makes only 0.3% to 0.8% of sweat. The sweat may therefore be regarded as the most dilute human secretion. The literature regarding the chemistry of sweat is enormous and so conflicting that one assumes an inadequacy of technique and a multiplicity of factors. One of the chief reasons for the discrepancies reported seems to be the difficulty of collecting sweat. The following three reasons are:

- Prevention of evaporative loss of water is more difficult than one might expect. High concentrations of constituents may therefore be suspected of having resulted from evaporation of sweat. When total body sweat is collected, checking the amount obtained against the loss of body weight is most commendable.
- Contamination of sweat samples with other substances present on the skin may be another cause of technical error.
- Concentrations of constituents vary considerably with changes in the rate of secretion.

2.1.1. Inorganic Constituents

The results of investigations on the inorganic constituents of human sweat reported are shown in Table 4.1.

Table 2.1: Inorganic Constituents MGM per cent [10]

Constituent	Amount [mg%]
Cl	36 - 995
Na	17 - 400
K	7 - 145
Ca	0.3 - 11.8
Mg	0.02 - 3.32
P	0 - 4.8
SO_4	4 - 17
I	0.0007
Cu	0.006
Mn	0.006
Fe	0.064 - 0.2

Chloride & Sodium: There is some evidence that Cl^- levels in sweat can be utilized to predict hormonal changes and therefore ovulation [12], but such correlations are more likely just a measure of how hormone levels can effect sweat response to external stimuli (e.g., stronger sweat response = higher sweat rate = higher Cl concentration). Currently, there are two unequivocally important uses for monitoring Na^+ and Cl^- in sweat. Cystic fibrosis is characterized by increased Na^+ and Cl^- sweat concentrations; this forms the basis of newborn early screening programs. Cystic fibrosis impairs lung function, which makes it is conceivable that this condition could lead to decreased oxygenation, especially during exercise and an increase in anaerobic metabolism leading to higher lactate levels [13] [14].

The second reason why it is valuable to measure Na^+ and Cl^- in sweat is because the concentrations can be used as an indirect measure of sweat rate utilizing the trends shown in Figure 2.3. Measuring sweat rate is important for improved measures of biomarkers whose concentrations are sweat rate dependent and is important for measuring the effective sampling interval for biomarkers [13]. Though not a good indicator of fatigue, Na^+ and Cl^- can be used to determine hyponatremia, hypokalemia, muscle cramps and state of hydration [4].

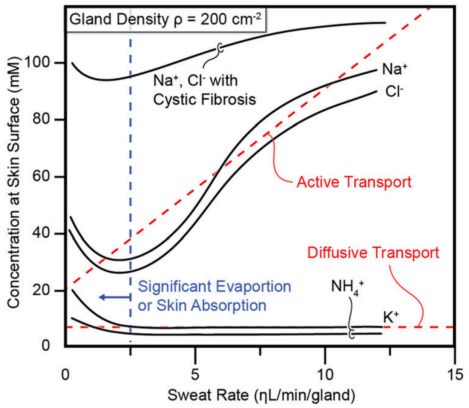

Figure 2.3: Biomarker surface concentration dependence upon sweat rate. It is speculated that increased solute concentrations at very low sweat rates are due to evaporation and fluid absorption on the skin [13]

As seen in Table 4.1, the concentrations of sweat chlorine reported by various investigators vary from 0.036 to almost one per cent. The higher values may be suspected to be a result of evaporative errors

as mentioned earlier. However other factors must affect concentration. The following consideration will be given to those factors which govern the content of chlorine. It will be noted that some of the factors are not only significant to chlorine, but also to other constituents of sweat.

1) The Rate of Secretion: It is well known that the concentration of the constituents of most secretions vary with the rate of secretion. It can be taken as a general rule at least for thermal sweating over the general body surface that sweat chloride concentration varies proportionally to the rate of sweating. So it is also possible to use Na^+ and Cl^- as an indirect measurement of sweat rate.

2) Regional Differences: That the chloride concentration varies in samples obtained from different parts of the body has been noticed by several investigators. The chloride concentration becomes progressively smaller in the order of the neck and chest; the abdomen, back and forehead; and the upper arm, thigh, leg and the back of the hand.

3) Skin Temperatures: Masui [15] found that the amount of chloride in sweat was large on the area of the skin where sweating was profuse, and small on that with moderate sweating even when the skin temperatures of these areas were the same. The rate of sweating may change proportionally to changes in the skin temperature, and the correlation between the latter and the chloride concentration seem to be a secondary consequence of changes in the rate of secretion.

4) Salt Intake: Many previous investigators claimed that the chloride content of sweat exhibited no correlation with the intake of chloride, while others, including Ladell, Waterlow and Hudson [16], pointed out that it was decreased by salt deficiency and increased by high salt intake. At least it seems certain that the salt content of sweat is reduced in salt deficiency. Locke, Talbot, Joncs and Worcester [17] observed the effect of varying the intake of sodium chloride and potassium salts. Water intake exerts little effect on the rate of sweating. However, it was reported by several investigators that the chloride concentration of sweat varied inversely with the supply of drinking water.

5) Adrenal Cortex: The levels of Na^+ and Cl^- in sweat appeared to reflect the degree of activity of corticoids which affect electrolyte metabolism. Patients with untreated Addison's disease showed concentrations of sodium and chloride in sweat far in excess of the highest normal values (90 to 123 mEq per L). In two cases of proved adrenal cortex carcinoma, one of Cushing's syndrome and the other of adrenogenital syndrome, concentrations of sodium and chloride in the sweat were extremely low (2 to 14 mEq per L). From these results they proposed that the concentration of chloride or sodium in thermal sweat can be used as an index of the function of the adrenal cortex concerned primarily with electrolyte metabolism.

Potassium: Potassium concentration in sweat is proportional to blood concentration or higher and is independent of sweat rate [10] [3]. It can be assumed that the sweat K^+ is derived from the K^+ accumulated in the gland cells and will be discharged as soon as secretion begins. With increase in secretory activity, Na^+ may enter the gland cells, and K^+ may partly be replaced with Na^+. The K^+ concentration in the gland cells is gradually reduced and in turn the sweat K^+ concentration falls. On the other hand, it may also be assumed that the blood supply of the sweat glands relative to their needs is low in the initial stage of sweating and that the discharge of K^+ is accelerated by the relative hypoxia. However the high K^+ concentration at the beginning of sweating seems to be ascribable at least in part to washing out of the K^+ of the epidermis [10].

From an applied perspective, K^+ in plasma predicts muscle activity. Excessive loss of sodium and K^+ in sweat could indicate hyponatremia, hypokalemia, muscle cramps or dehydration [18] [19] [3] [10].

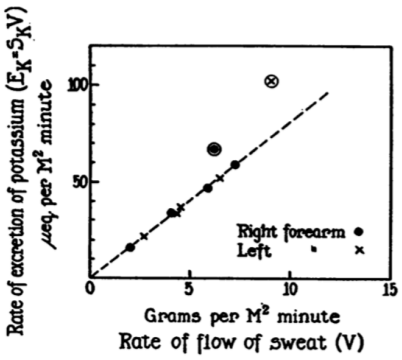

Figure 2.4: Relation Between the Rate of Excretion of Potassium the Sweat and the Sweating Rate [20]

Calcium: Calcium is much more dilute in sweat than blood plasma. The sweat Ca^{2+} concentration seems therefore to vary with the rate of sweating similarity to K^+. The skin seems to be an important channel for elimination of Ca^{2+}. It has been reported that about 15 per cent of the total output of Ca^{2+} under non-sweating conditions, and about 30 per cent under sweating conditions, may be eliminated through the skin, i.e., the cutaneous output of Ca^{2+} may far exceed that in the urine under some conditions.

Magnesium: The magnesium contents of sweat reported by various investigators vary considerably so that a standard value cannot be given. Changes in concentration with changes in rate of sweating however seem to be similar to those of K^+ and Ca^{2+}.

Phosphate: The presence of phosphate in sweat has been doubted by several investigators. However, Talbert et al. [21] found an appreciable, but variable, amount of phosphorus in sweat of both organic and inorganic origin. The character of the diet seems to have an appreciable influence on the amount secreted. A diet low in phosphate yields usually 1mg% to 2 mg%, while a diet known to be high in phosphates like asparagus, spinach, fish and eggs will give readings from 2.5mg% to 3.5 mg%. The intake of 15 g of Na_2HPO_4 yields similar results.

It is well known that the concentration of inorganic phosphate in the protoplasm is low relative to that of phosphate esters, and it has been reported that the greater part of the intracellular phosphorus is nondializable. Accordingly, little discharge of the intracellular phosphates into the sweat would be expected. These phosphates may play a role as suppliers of energy for secretion, but this is uncertain.

Sulphate: It has been reported that sweat sulphate is not influenced by the sulphate concentration in blood plasma. In some experiments high values for sulphate were found in sweat during the initial period of sweating and were ascribed to mixing of sulphate derived from the epidermal surface.

Iodine: The iodine balance in normal subjects and patients with thyroid disease has been studied by several investigators and the importance of the skin as an avenue of excretion in attaining a true balance of iodine and the increase in its dermal loss in exophthalmic goitre have been recognized. But the dermal excretion in these investigations was obtained after repeated washing of the body and underclothes and the iodine content of sweat was not determined.

Spector et al. [22] observed the effect of environmental temperature on the excretion of iodine by normal subjects. A single dose of 2 mg of KI increased the average concentration of iodine in sweat, while fourteen daily doses of 2 mg of KI did not produce any significant additional increase. Profuse sweating increased dermal losses of iodine at high levels of iodine intake, but at low levels no consistent or considerable effect was observed. At least 75% of the total iodine lost from the body was excreted through the urine.

Iron: Mitchell and Hamilton [23] who found relatively high values of iron in sweat considered that the skin and sweat glands are important excretory organs for iron. However, according to voluminous data obtained by iron balance studies, a considerable loss of iron through the skin is difficult to admit. According to Green et al. [24], the iron content of ”cell poor” sweat was negligible while a high concentration was found in ”cell rich” sweat. This suggests that the iron loss is no essential function of

the process of sweating, but associated primarily with desquamation. On the other hand, no change in the iron loss by large intake of iron has been shown experimentally.

2.1.2. Nitrogen Compounds

Table 2.2 shows the reports on nitrogen compounds in sweat. The amount of total nitrogen contained in sweat has been variously reported, i.e., from 17 to 196 mg% as shown in this table. Such conflicting data may have resulted in part from differences in methods of determination, but more considerably by contamination with debris of the superficial epidermis.

In temperate climates, an average adult with occasional slight sweating may lose 0.3 g of nitrogen or less daily through the skin and its amount may increase with augmentation of sweating.

Table 2.2: Nitrogen Compounds (MGM per cent) [10]

Constituent	Amount [MGM per cent]
Total Nitrogen	17 - 196
Non-protein	66 - 108
Amino acids	1.1 - 10.2
Ammonia	2.5 - 35
Urea	8.4 - 128
Uric acids	0 - 1.2
Creatinine	0.2 - 1.9

Amino acids: The concentration of amino acid nitrogen in sweat varies over a wide range, i.e., from 1.1 to 10.2 mg%. It is high in the initial stage of sweating when the secretion is scanty, and low when it becomes profuse. It again increases when sweating subsides by lowering room temperature. In general, therefore, the amino acid content in sweat varies in inverse relation to the rate of secretion. An experiment showing this relationship is illustrated in Figure 2.6. The concentration of amino acid nitrogen in sweat falls far below its level in blood plasma as long as sweating is profuse and exceeds the latter only when sweating is scanty. Since amino acid concentration of skin is more than twice that in plasma, the values in sweat are always lower than those in the skin.

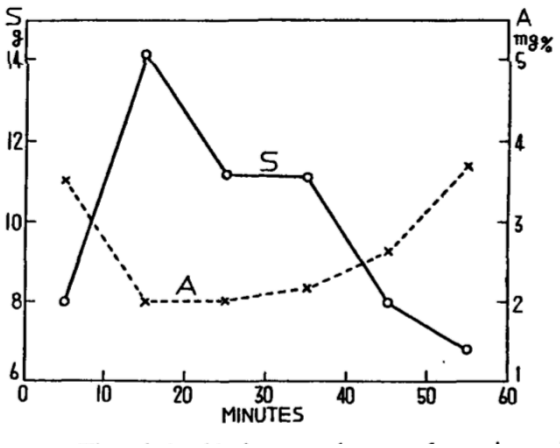

Figure 2.5: The relationship between the rate of sweating and the amino acid concentration of sweat. S: amount of sweat collected from one forearm per ten minutes. A: amino acid in mg% [10]

Ammonia: The ammonia concentration in sweat Is high in the initial stage of sweating and lowers with progress of sweating. It might be imagined that the discharge of ammonia in sweat is of significance in the neutralization of acid and in the economy of base as is the case with the kidney. Another study

conducted by Alvear et al. 2005 [25] shows that during a rugby match, the sweat ammonia of the players increased significantly and significantly reduced 24h after the match.

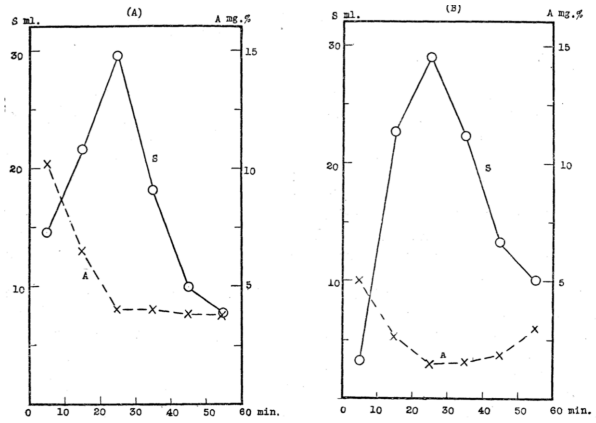

Figure 2.6: Relationship between ammonia (A) content of sweat (S) and the rate of secretion. Two examples of experiments are shown in this figure [10]

Urea: Urea is produced in liver tissue from ammonia and carbon dioxide and sweat has also been shown to contain considerable amounts of urea coming from the plasma [26]. Urea is a nitrogen-containing metabolite typically excreted by the kidney but is found to be alternatively excreted through sweat glands. Urea partitioning into sweat has not been fully confirmed but ideas of passive transport across glands from blood into sweat precursor fluid has been a common speculation and emphasized by urea's diffusibility [10] through membranes as well as its ratio relationships to plasma [25]. Another theory of urea partitioning is possible metabolism by the sweat glands or other means such as Urea Transporter-B [3]. During measurements, there will be a very high value of urea found in the initial sweat. This may be due to washing out of urea in the epidermis. The concentration in sweat always remained higher than its level in the blood, because the changes in sweat urea may be due to re-absorption of water in the sweat duct. In the study of Alvear et al. 2005 [25] similar to ammonia, urea also increased during the rugby match. However the urea concentration was significantly reduced 48h after the match, hence possibly being a slower process than ammonia due to the diffusion process.

Creatinine: The creatinine content of sweat is considered by most investigators to be similar to that in blood plasma. According to Ladell [27], the creatinine concentration is more than 1.0 mg% in early samples of sweat and falls to 0.3 mg% or less when the sweat rate is greatest. The sweat creatinine appears not to be linked with the level of creatinine in the blood. [10].

2.1.3. Sugars and its metabolites

Glucose: sugar content of sweat is extremely low (between 1 - 11 mg%) and it was found by Itoh and Suchi [28] that it was high at the initial stage of sweating and fell with the progress of sweating. Sweat glucose is reported to be metabolically related to blood glucose [29]. On the contrary Lobitz and Osterberg (1947) [30] found by their microanalytic method that the palmar sweat showed no change in the concentration of reducing substances with changes in the rate of secretion nor with the intake of glucose.

Table 2.3: Sugars and its Metabolites (MGM per cent) [10]

Constituent	Amount [mg%]
Glucose	1 - 25.6
Lactic acid	71 - 300
Pyruvic acid	0.9 - 6.9

Sweat Lactate: In contrast, a large amount of lactic acid, far higher than that in blood, is contained in

sweat. It was once claimed that lactic acid in sweat increases in proportion to the severity of muscular exercise and that its removal by sweating is important for protecting the kidneys. The overwhelming majority of the literature indicates that blood and sweat lactate concentration are independent of one another since lactate within sweat is entirely a by-product of sweat gland metabolism, and evidence from a wide variety of studies can be used to support this view [10] [31] [32] [33] [34] [25] [35]. The sweat lactic acid seems therefore not to be diffused from blood, but produced in the eccrine glands. However, according to [36] there is a correlation in changes of lactate concentration in blood and in sweat during exercise. This is possibly due to the skin temperature heating up for the relatively short period during the experiment, which may not imply that the correlation will be the same when conducted over a longer period of time, when the body acclimatizes during a tour cycling or marathon.

The sweat lactic acid concentration is high at the initial stage of sweating, does not change much later, but more or less falls when sweating becomes very profuse. It has been reported that lactic acid in sweat is reduced by acclimatization to heat and that it undergoes some seasonal variations [14] [25].

According to Derbyshire (2012) [14] sweat lactate can potentially serve as a sensitive marker of pressure ischemia. Pressure ischemia describes the condition of reduced oxygen perfusion in tissue due to an applied force. This can in turn lead to decubitus ulcers if perfusion remains low for an extended period of time.

Pyruvic acid: The pyruvic acid concentration in sweat is very high, four to ten times as high as its level in the blood at the initial stage of sweating, but it rapidly decreases with increase in the rate of sweating so that its concentration soon approaches the blood level [10].

The fact that glucose, lactic acid and pyruvic acid are discharged in high concentration in sweat at the initial stage of sweating and diminish with progress of sweating seems to suggest that the utilization of sugar by the sweat glands increases progressively with progress of secretion. On the other hand, the very high concentration of lactic acid and pyruvic acid in the initial sweat may partly result from washing out the acids present in the sweat ducts or in the epidermis. It has been demonstrated that large amounts of both the acids are contained in the epidermis.

2.1.4. General view

The essential constituents of sweat may be classified into the following groups in view of the relationship of their concentrations to those in the blood plasma and of the changes in their concentrations owing to changes in the rate of sweating.

1. The constituents, the concentration of which increases proportionally to the rate of sweating, yet remains always below the level in plasma:

   - Sodium
   - Chloride

2. Those showing an eminent inverse proportion between their concentrations and the rate of sweating:

   - Glucose
   - Amino Acids

They are the substances important as energy sources for the gland cells. That their concentrations in sweat fall with increase in the rate of secretion may be considered as a result of increased utilization by the gland cells

3. Those where the concentrations are high during the initial stage of sweating and fall with increase in the rate of sweating. They may be classified into three groups with respect to their concentrations relative to plasma.

a) Those which are more concentrated in sweat than in plasma:

   - Potassium
   - Ammonia

- Lactic Acid
- Pyruvic Acid

All these are substances which are either contained or produced in the gland cells in quantity and discharged from the cells into sweat. They are also contained in the epidermis in large quantities and their high concentrations in the initial sweat may possibly result from mingling of the substances into sweat from the epidermis.

b) Those with similar concentrations in sweat and plasma: urea

- Urea

c) Those with lower concentrations in sweat than in plasma:

- Calcium
- Magnesium
- Creatinine

From the above circumstances it may be considered that the sweat during the initial stage of sweating contains substances admixed from skin tissue other than the sweat glands, whereas the sweat obtained during more profuse sweating may contain only substances either secreted from, or filtered through, the gland cells. The representative concentrations of the essential constituents of sweat are therefore compared with their concentrations in plasma in Table 2.4.

Table 2.4: The Average Concentration the Sweat Constituents in Sweat and in Plasma (MGM per cent) [10]

Substance	Sweat	Blood Plasma
Cl	320	360
Na	200	340
K	20	18
Ca	2	10
Mg	1	2.5
Urea-N	15	15
Amino Acid-N	1	5
Ammonia	5	0.05
Creatinine	0.3	1.5
Glucose	2	100
Lactic Acid	35	15

There are also reports of (water-soluble) vitamins in sweat. However it seems almost certain that the loss of vitamins in the sweat is not a significant factor in depleting the body's stores according to Kuno (1934) [10]. Even under severe conditions that necessitate a daily loss of 10 to 15 liters of sweat, excretion of vitamins is considerably greater in the urine than in the sweat.

3

Ammonia

In chapter 2, different constituents in sweat were mentioned and it was explained that ammonia concentration is one of the constituents which correlates with muscle fatigue. This chapter will go further in depth about ammonia.

In the purine nucleotide cycle (PNC) Figure 3.1, an enzyme called myoadenylate deaminase (MAD) catalyzes the irreversible deanination of the adenosine monophosphate (AMP) to inosine monophosphate (IMP). Resynthesis of AMP occurs by the sequential action of adenylosuccinate synthase and adenylosuccinase. Necessary for the purine nucleotide cycle are aspartate and guanosine triphosphate (GTP), while furmarate, guanosine diphosphate GDP, organic phosphate, and ammonia are formed [37] [38]. The purine nucleotide cycle is known to be active during exercise and especially during ischemic exercises [39] [40]. Though there is a difference between ischemic exercise and anaerobic exercise, in both exercises will result into an oxygen supply shortage in the muscle fibres.

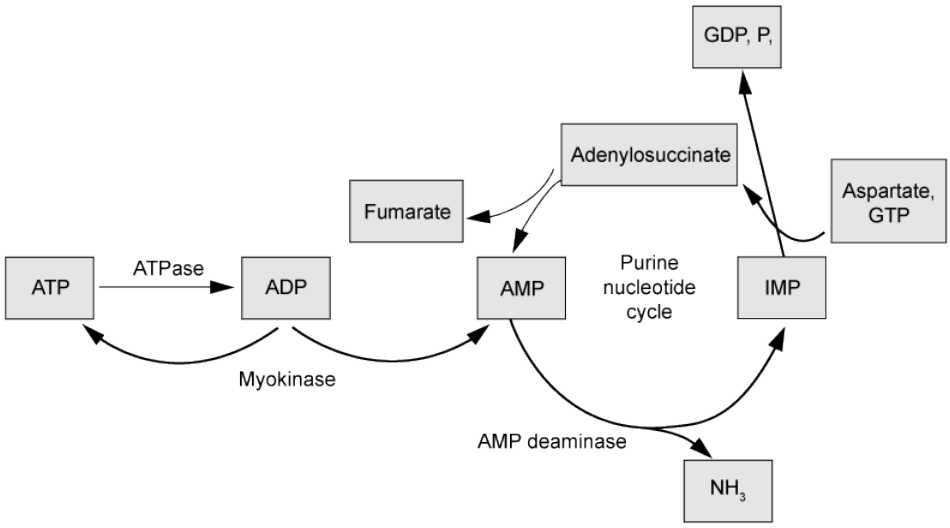

Figure 3.1: Main characteristics of the purine nucleotide cycle

Similar to lactate, ammonia will also flow into the blood plasma. However, it is likely that ammonia diffuses from the blood into the sweat glands [41]. Due to blood ammonia resulting from PNC activity of the muscles, the determination of the levels of this cation in plasma provides extremely relevant physiological information related to the metabolic state of the individual [34].

The ammonia excretion via sweat and ammonia production of exercising muscles is in the same order of magnitude. However, another possible source of ammonia in sweat could be the PNC activity during

lactate production in the gland cells [34]. Most investigators found that the concentration of ammonia in sweat range from 0.5 mM and 8 mM [13] with an average concentration amount to 3.0 mM. This means that the concentration of ammonia in the sweat is 80-150 times higher than in the blood [38]. The amount of ammonia in sweat produced by this PNC activity is far too low to explain higher ammonia concentration in sweat in relation the blood [34]. Thus if there is a contribution of ammonia in sweat through PNC activity in the gland cell, then it is negligible in comparison to the ammonia content in sweat. Another source of ammonia is could be the result of urease activity of skin bacteria, possibly *Staphylococcus epidermicus* [42].

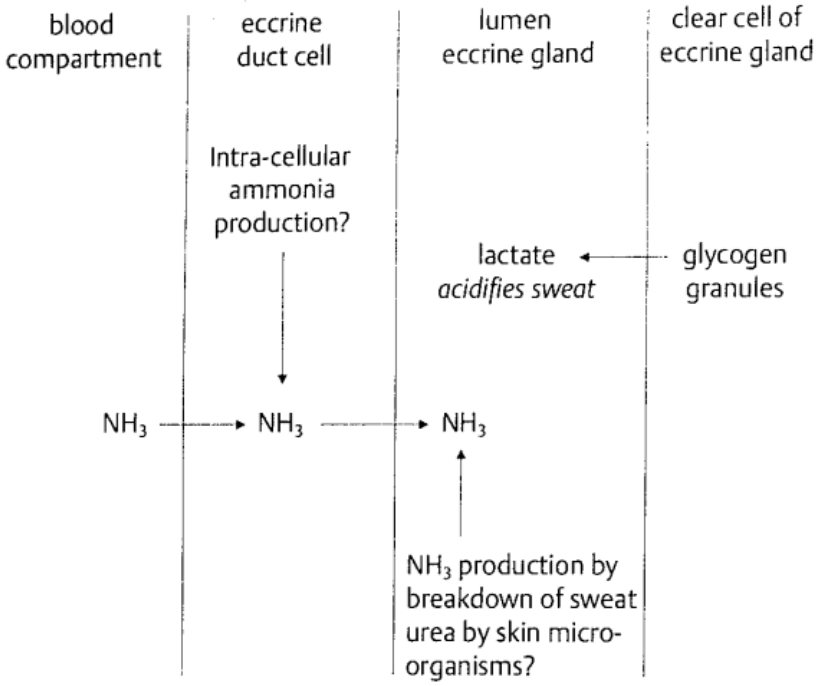

Figure 3.2: Diagram of the hypothetical routes of ammonia to the lumen of the eccrine sweat gland [34]

The ammonia concentration also depends on the environmental pH. In the human body the ammonium ion is formed from ammonia gas and vice versa in an equilibrium reaction:

$$NH_3(g) + H^+ \leftrightarrow {NH_4}^+ \tag{3.1}$$

At a physiological pH of 7.3 99% is in the form of ${NH_4}^+$ and 1% in the form of NH_3 (Figure 3.3), the so called 'free ammonia' [43]. However in most paper, the term ammonia refers to the total ammonia concentration, i.e. $NH_3 + {NH_4}^+$.

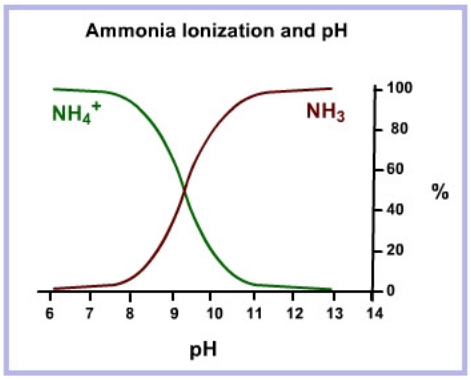

Figure 3.3: Ammonia ionization and pH

The clinical significance is not clear, however a correlation between exercise and the ammonia concentration in plasma has been found [44] [38] [25] [40]. Alvear, *et al.* [25] and Guinovart, *et al.*[44] conclude that there is an increase level of sweat ammonia when the subject increases the workload (Appendix B & Figure B). However, Ament, *et al.* [34] (Figure B) shows a decrease in ammonia concentration during incremental workloads. This was also mentioned in the paper of Alvear, *et al.*. He explained this effect by an increasing sweat rate for higher load of intensity, which results in a dilution effect of the ammonia concentration in the paper of Ament, *et al.*, which confounds their results. Zoerner, *et al.* [45] also showed there is a decrease of sweat ammonia concentration. They explain that Guinovart, *et al.* although they show an ammonia increase during exercise for different intensity load, during continuous measurement on skin it is possible that an accumulation of ammonia take place, whereas in the work of Zoerner, *et al.*, the sensor is rinsed with destilled water before each measurement of sweat samples. Also due to body temperature increase, possible evaporation of liquid can cause accumulation of ammonia. B shows the ammonia trend of the articles which were mentioned. Though it is not completely clear, both parties does conclude the relationship between fatigue and sweat ammonia concentration.

Additionally, it has been shown that diets with low levels of carbohydrates may lead to temporary increased levels of ammonia in plasma, which is sometimes evidenced as an ammonia smell in sweat [8]. Last, but not least, since the liver converts ammonia to urea prior to its excretion, high ammonia levels can be used as markers of hepatic disorders, such as hepatitis or cirrhosis. All in all, monitoring the levels of ammonia may provide a wealth of information, which ranges from the improvement of the sport performance and monitoring metabolic state to the screening of the health status of individuals.

4

Measuring Methods

In chapter 2, different constituents in sweat were mentioned. And as explained in chapter 3, ammonia concentration is one of the potential constituents which has a correlation with muscle fatigue. This chapter will go further into how sweat is collected and discuss the different methods of measuring ammonia concentrations in sweat.

4.1. Sweat Collection

Various methods of sweat collection are used for chemical analysis. The most common method of sweat collection is to enclose one extremity in an impermeable bag, or to cover an area of skin with a chamber, and to collect the sweat streaming into it, while the sweat remaining over the skin is picked up with absorbent paper. In such cases, it must be kept in mind that the avoidance of evaporation of sweat during the procedures is far more difficult than expected. The vapor tension of the air in the bag being very high, water is apt to escape from minute orifices, and some evaporation after opening the bag is unavoidable [10].

For more local sweat collection, the *Macroduct Sweat Collector* is a unique disposable plastic device having a shallow, concave under-surface. The Macroduct is a commercial device which collects collects the sweat in the spiral tubing as the collector makes contact with the skin, and the small pinhole at the bottom allows the sweat to go through the tube. A small amount of blue dye allows easy monitoring of the accumulated sweat volume. After a sufficient volume of sweat has accumulated, a sweat dispenser, or blunt needle on a tuberculin syringe is connected to the open end of the tubing. The tubing is then uncoiled from the body of the Macroduct and severed at the point of attachment to a device that measures sodium and chloride concentration which as previously mentioned is served as a diagnosis of cystic fibrosis.

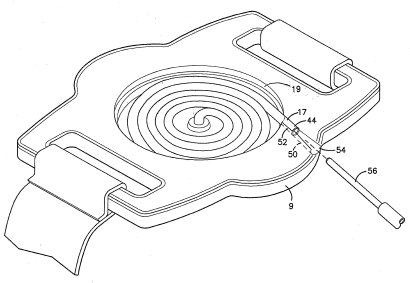

Figure 4.1: Macroduct

Figure 4.2: Macroduct

4.2. Monitoring Methods

4.2.1. Ion-Selective Electrodes

All recent studies that measure inorganic constituents in sweat, on a wearable device, does so by using ion-selective electrodes (ISE) [4] [46] [19]. These sensors are time efficient and also relatively cheap to use. In ISE method one electrode is responsible only for one element so for a large number of nutrients or elements we have to use different-different electrode according to property of elements[47]. However, the widespread use of chemical sensors has been complicated by several factors which are difficult to overcome. These include sample generation, collection and delivery, sensor calibration, wearability and safety issues [48]. Guinovart *et al.* [44] developed ammonium-selective electrodes by means of screen printing on flexible foils that can be directly stuck to the skin surface as a tattoo including the reference electrode. However, interfering ions like potassium, K^+ and sodium, Na^+, which are main components in sweat, have to be considered as species that can influence the proper acquisition of the ammonia level [4] [49] [45]. Additionally, while a relatively simple method to monitor chemicals, it is not suitable for longterm uasage. After an extended period of uses, the accuracy of the electrode will diminish due to the degradation of these electrodes. Also the use of electrode requires skin temperature monitoring to compensate for and eliminate the influence of temperature variation in the readings of the chemical sensors [4].

Figure 4.3: Vernier: Commercially available Ammonia Ion-Selective Electrode

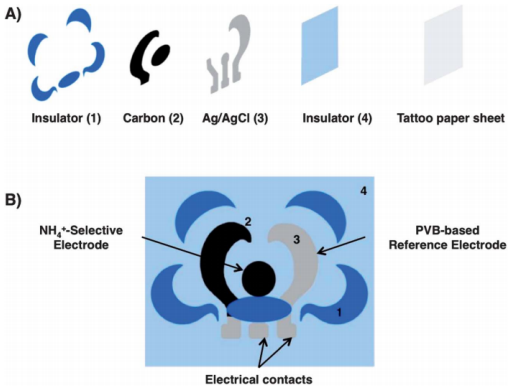

Figure 4.4: Layer-by-layer fabrication of the potentiometric tattoo sensor. (A) The process starts by adding a release layer in a tattoo paper sheet. Ag/AgCl, carbon and insulator layers are screen-printed onto the release layer to get the flower tattoo. (B) Both reference and ion-selective membranes are deposited onto the electrodes area

4.2.2. Enzyme-Based Sensors

The monitoring using enzyme-based sensors is based on oxidase [4] [50]. Gao, *et al.* developed a sweat sensor which contains multiple sensor which includes, salts, glucose and lactate. Glucose and lactate sensor output are based on glucose and lactate oxidase immobilized within a permeable film of the linear polysaccharide chitosan. Thus, the electrode-based sensors utilized specific enzymes, glucose oxidase and lactate oxidase, suspended in a support matrix, and measured oxygen as a correlative marker for glucose and lactate levels. For ammonia, the enzyme alanine dehydrogenase (AlaDH) can be used [51]. While demonstrating excellent sensitivity and specificity, the complexity of current enzyme-based sensors have limited potential for persistent long-term monitoring applications due to enzymatic lifetime and stability [52] [53]. Another major limitation of oxidase enzyme-based biosensors is the dependence of enzyme activity on the background oxygen concentration in sample solutions which causes the problem of baseline drift during long-term monitoring [53].

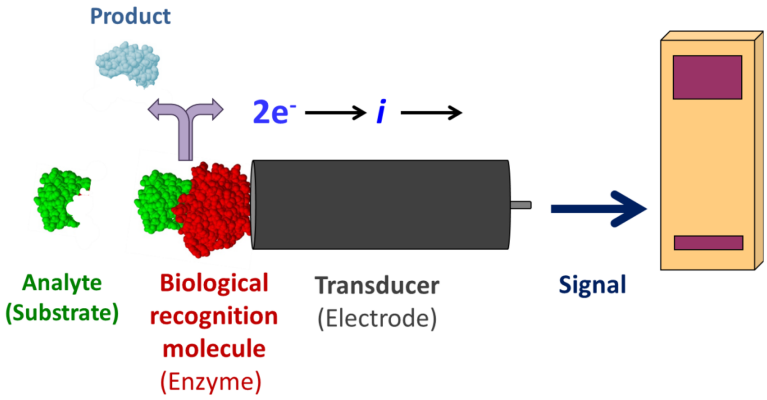

Figure 4.5: A typical design of an enzyme modified electrochemical biosensor

4.2.3. Colorimetric sensor

It is also possible to use a chemical specific dye which changes colour and determine the concentration based on the colour intensity. *Morris et al.* (2009) [54] developed of a textile based fluid handling system for real-time monitoring of sweat pH. It collects the sweat from the skin surface and wicks the sample through a predefined channel to the sensing area. To maintain continuous fluid flow a super absorbent material was attached at the end of the fluidic channel (Figure 4.6).

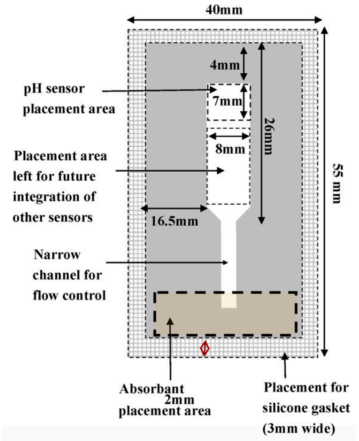

Figure 4.6: Layout of fluid handling system and position of pH sensor

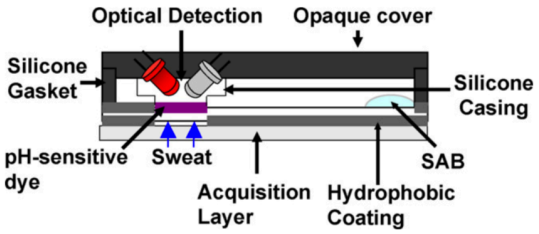

Figure 4.7: Illustration of pH sensor and optical detection system

Sweat pH monitoring involves using a pH sensitive dye which changes colour depending on the pH

of the sweat. This colour change is detected by diffuse reflectance measurement using an emitter-detector LED technique. To obtain quantitative pH measurements a paired emitter-detector dual LED configuration was used as seen in (Figure 4.7). The detector LED is reverse biased at a specific voltage. The photo current generated upon incident light then discharges the LED at a rate that is proportional to the intensity of light reaching the detector

4.2.4. Near-Infrared Spectroscopy

The last possible method of ammonia monitoring, is using near-infrared spectroscopy (NIRS). Wang (2016) [55] developed a U-shaped Whispering-Gallery Mode-based (WGM) optical fiber sensor for real-time monitoring of blood sugar levels. This is done by using a U-shaped WGM-based optical fiber sensor with diameter was 1.5mm, because the literature survey reveals that the use WGM sensors with diameters smaller than 1.5mm is unable to measure aqueous solutions of glucose.

During the experiment, measurements of aqueous solutions of glucose with concentrations ranging from 6% to 38% were conducted. The experiment undertake measurement spacing was 4%. These experimental results showed that the transmission losses in the U-shaped WGM sensor spectra were altered with changes in glucose concentrations. The experimental results in Figure 4.11 show that the sensing transmission loss sensitivity for the concentrations of the aqueous solution of glucose was 0.085 dB/%, while the linearity (R^2) was 0.925.

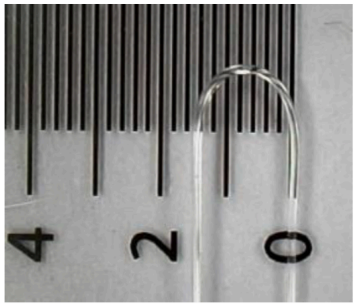

Figure 4.8: Photograph of the small WGM optical fiber sensor (radius=0.75mm).

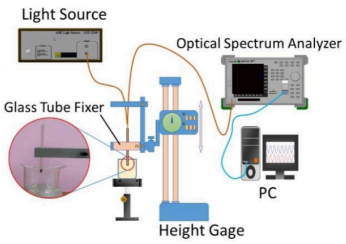

Figure 4.9: The experimental set-up for measuring glucose water concentrations with the small U-shaped WGM-based optical fiber sensor.

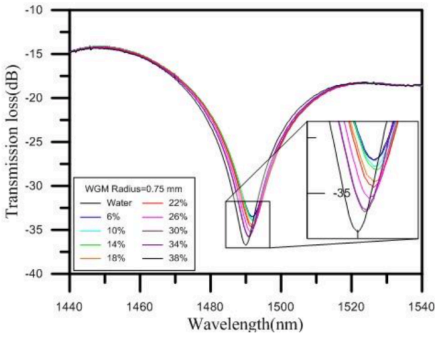

Figure 4.10: Spectrogram of the aqueous solution of glucose concentration sensing results

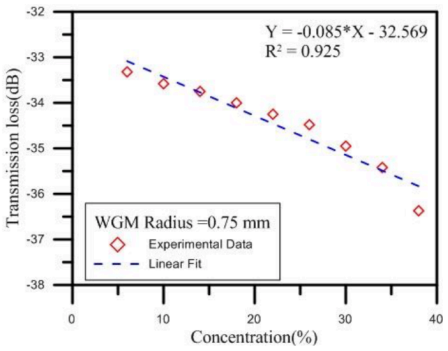

Figure 4.11: Transmission loss diagram of the aqueous solution of glucose concentration sensing results.

The transmission loss increased as the glucose concentration percentage was increased. These results demonstrate that the proposed U-shape WGM sensor has good potential for high-sensitivity glucose concentration sensor applications [55]. The main advantage of this measuring method is that it converts an optical signal into electrical signals, hence many factors which may influence measurements in the previous methods such as temperature, pH and oxygen have no influence on measurements using

NIRS. However disadvantage is that it is rather complex and there are few studies done in sweat applications.

Determining concentration of any constituent in sweat using near infra-red spectroscopy is very challenging yet attractive. At the first glance, bodyfluids (i.e. sweat) are very close to the spectrum of water shown in Figure 4.12, since it consists 99% water. The remaining 1% consist salts, nitrogen-based compounds etc which are already mentioned in chapter 2.

A related study was conducted by Czarnik *et al.* (1999) by using NIRS to determine protein and fat concentration by looking at spectral changes in milk Figure 4.13. The NIR spectra of milk offer a good opportunity to challenge the analysis of NIR spectra of biological materials consisting of complex but basic molecules [56]. In this study it was concluded that the bands between 2000 nm and 2100 nm may unambiguously assigned to amide B/II combination [56] [57] [58] (basically N–H stretching combined with N–H bending). A slice spectrum was extracted in this study at 2048 nm, a wavelength which strongly correlates the N-H combination vibration with other bands. Chung [58] found Bands above 2300 nm are assigned for C-H combinations.

A broad band near 1450 nm is assigned to the combination of O-H symmetric and asymmetric stretching modes of water [59] [56], while an intense feature near 1930 nm is due to the combination of OH bending and symmetric stretching modes of water [56].

Table 4.1: Proposed assignments of bands observed in analyzed 2D maps attributed to fat and protein species [56]

Band Position [nm]	Assignment
1250 - 1255	First overtone of amide A + amide II
1584	First overtone of amide A
1638	First overtone of amide B
2038 - 2075	Amide A + amide I
2100	Amide B + amide I
2124	Amide B + amide I
2160	Amide B + amide II
2186	Amide A + amide II

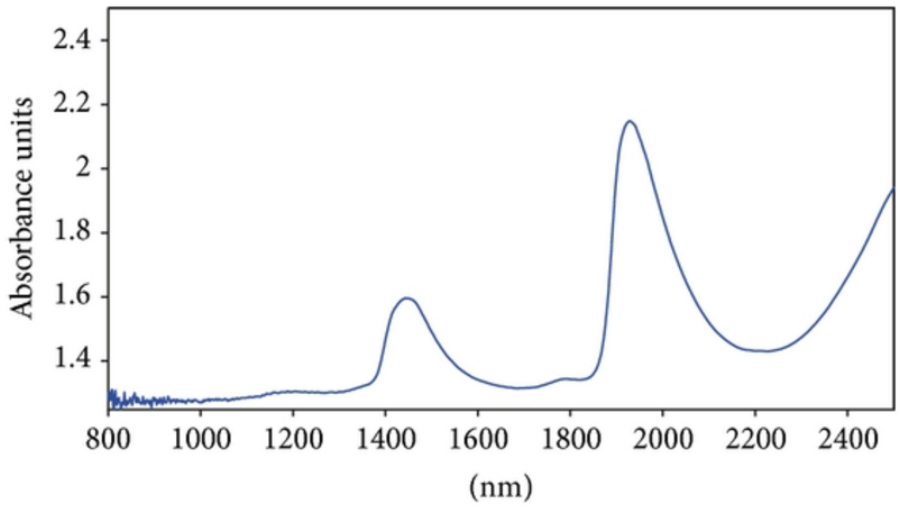

Figure 4.12: Water spectra when the path length is 1, 2, 5, or 10mm [60]

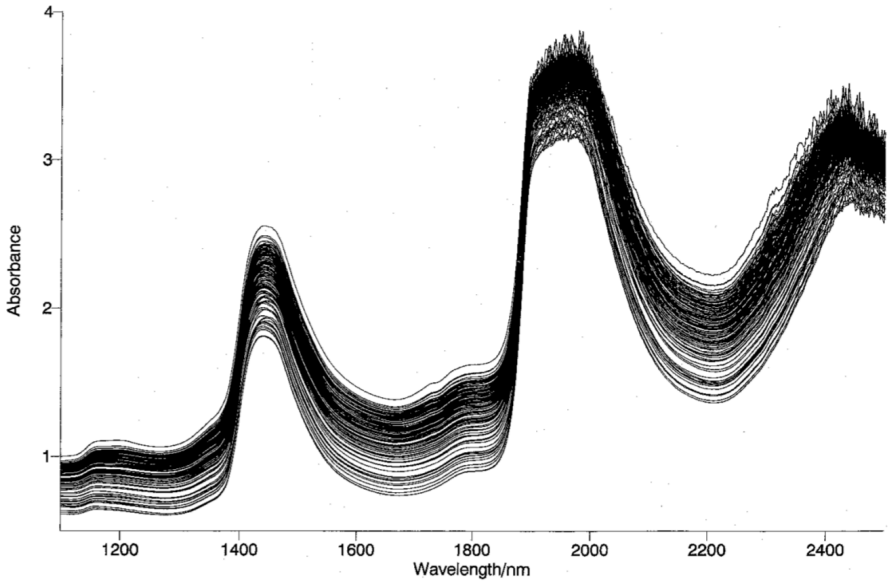

Figure 4.13: NIR spectra in the 1100 - 2500 nm region of 165 milk samples. [56]

Savsic 2001 [61] measured the concentration of fat, protein and lactose in milk by monitoring the partial least squares regression (PLS). He concluded that the there is no one specific wavelength which correlates to a molecule, but a range of different wavelengths, with the use of the PLS a predicted concentration of ammonia can be given.

Despite the benefit of using NIRS, thus far, very few investigations have been reported regarding dissolved ammonia in a solution. As mentioned earlier in chapter 4, while Wang [55] developed a optical glucose sensor, the tested samples only contained diluted glucose, whereas sweat contains multiple chemical. Additionally, the absence of a near-infrared spectroscope also disables an attempt to conduct research in acquiring more insight about this method. Due to lack of research done on the feasibility of using NIRS for sweat analysis, for the design of the sweat analysis, it is not possible at this time to measure ammonia through NIRS.

4.2.5. MOS Sensor

Due to lack of research done on the feasibility of using NIRS for sweat analysis, for the design of the sweat analysis device, an new method is introduced, namely measuring ammonia in a gas phase. The reason for this choice is because of the trend uncertainty of how ammonia concentration changes under anaerobic conditions. Measuring ammonia in gas phase removes the complexity of fluid transport to the sensor and cancels the influence of sweat rate which dilutes the ammonia concentration and give false values. Additionally, for all other measuring methods, the user must start sweating in order to start the measurements. In theory, because ammonia is less polar that water, it is possibly that ammonia can perspire in gas phase similar to how water can perspire in gas phase when during less intense activities. There is also a large variety in commercially available ammonia gas sensors in the car, industrial and chemical industry.

Gas sensors work by using a metal oxide layer which are also called metal-oxide sensor (MOS) Figure 4.14. The sensor element is typically heated to a few hundred degrees centigrade using a small restive heater. The equivalent circuit model described by Naisbitt et al. [62] defines three regions of the semiconductor: the surface, which interacts with the gas, the bulk, which is unaffected by it, and the particle boundary, which lies in between these two. The particle boundary is situated at a distance from any material exposed to the atmosphere equal to the Debye length: the distance into the sensor that chemical electrostatic effects can propagate, related to the material's physical properties. At high temperatures, oxygen atoms bond onto the boundary, extracting electrons in the process from the semiconductor's surface region. The oxygen either then directly reacts with ambient gases, or these

gases also bond onto the sensor, which causes more charge carriers to be withdrawn or injected into the surface region [63]. This changes its electrical conductivity locally; which leads to a change of its electrical resistance. The change of electrical (R_S) resistance can be calculated by connecting the sensor in a voltage divider circuit. The measured output voltage can be used to calculate the output resistance R_S.

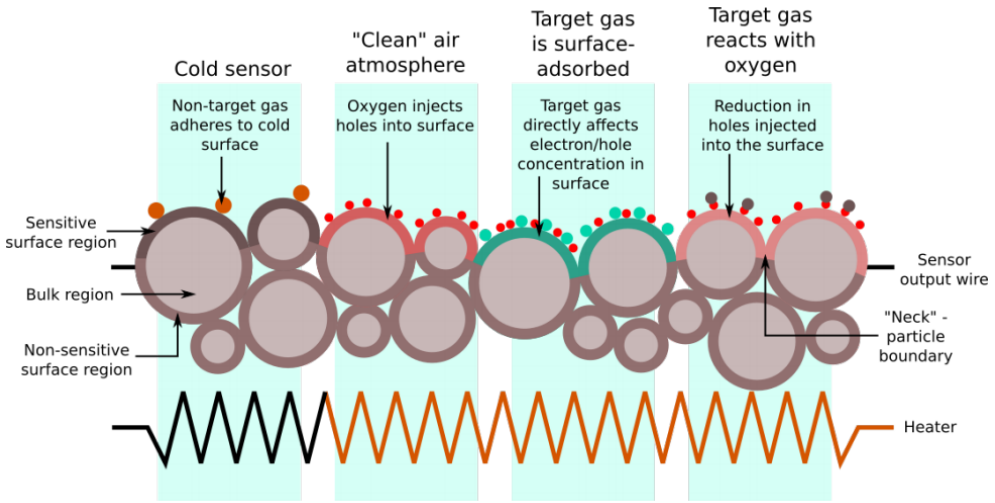

Figure 4.14: Diagram of the various types of interaction between atmospheric gases and an MOS sensor surface. In the leftmost region, the sensor is unpowered (and exhibits the base resistance). The three other regions of the diagram describe different processes that actually occur simultaneously to varying degrees. The sensor's output is the resistance across the whole of the sensor material, which forms a resistor network with contributions from both the bulk and surface regions (although the non-sensitive surface will have similar properties to the bulk). This model of the sensor material also explains the wide variation in base resistance between individual sensors of the same type, as the random nature of the surface geometry means an equally random network of resistances. This diagram is a two-dimensional representation of a three-dimensional material; in an actual sensor, the sensitive region is spread into the surface with a distance dependent on the grain size and arrangement resulting from the sintering [63]

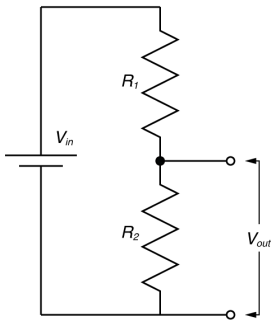

Figure 4.15: Voltage Divider; $R_S = R_1$ & $R_L = R_2$

$$R_S = \left(\frac{V_{in} - V_{out}}{V_{out}}\right) * R_L \tag{4.1}$$

The reason for using a MOS gas sensor is due to its large amount of commercially available devices which are available in very compact sizes. For the ammonia MOS gas sensor, MiCS 5914 sensor was chosen to due to its claimed range, size and affordability. Analyzing the modifications of the resistance

over time, compared with reference values, can give some information about variable gas concentrations. Data-sheet shown in Figure 4.16 is acquired by the manufacturer of the ammonia sensor.

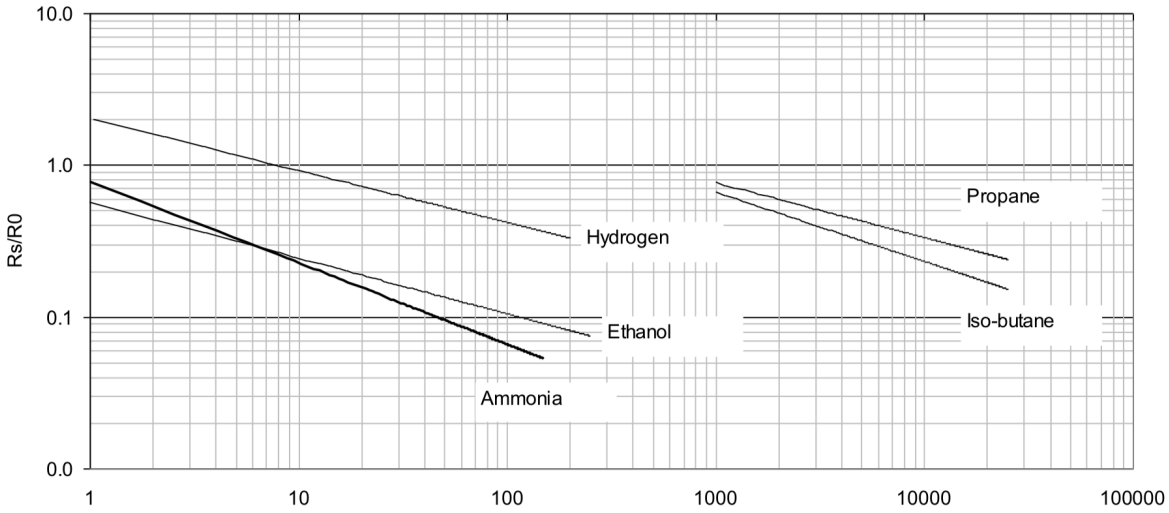

Figure 4.16: is shows the typical sensitivity characteristics of the sensor for several gases

As seen in the data-sheet, the sensor also reacts to other chemical compounds, however non of these compounds are expected to be present in sports application except for ethanol. However ethanol is expected to only be present in high quantity when the participant is intoxicated, hence the influence of ethanol is also ruled out since it is assumed that the participant would not be under the influence of alcohol during the use of this sensor.

Given the data-sheet is shown in a log-log diagram, the first objective is to get a trend line by first re-plotting the graph on a linear axis using *WebPoltDigitizer version 4.1* Figure 4.17.

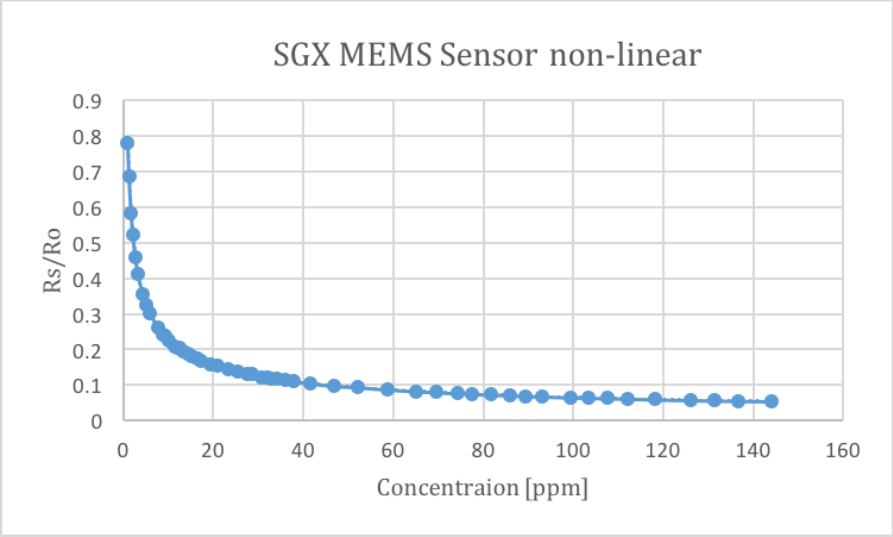

Figure 4.17: Data sheet on a linear axis

The resulting trend line of Figure 4.17 was determined by *Microsoft Excel 2010*:

$$\left(\frac{Rs}{Ro}\right) = 0.786 * (ppm)^{-0.539} \tag{4.2}$$

The trend line has a high correlation with the provided data from the datasheet ($R^2 = 0.99988$), which means little information is lost. In order to determine the ammonia concentration, we must first determine what R_0. The R_0 is the sensing resistance in air. The R_0 is calculated calibrating with air. According to Dutch Ministry of Health Welfare and Sport [64], the average ammonia concentration in air is 9 $\mu g/m^3$. Given the molar weight of 17.031 for ammonia, the concentration is 12.92 ppb.

$$\left(\frac{R_S}{R_0}\right) = 0.786 * (ppm)^{-0.539} = 0.786 * \left(12.92 * 10^{-3}\right)^{-0.539} = 8.1932 \tag{4.3}$$

By taking the measured average from Equation 4.1, which is 259.48 Ω and Equation 4.3 we can estimate the air sensing resistance R_0

$$R_0 = \frac{R_s}{\frac{R_s}{R_0}} = \frac{259.48}{8.1932} = 31.67k\Omega \tag{4.4}$$

Thus during measurements, given that R_0 = 31.67 $k\Omega$ and R_s being the sensor output resistance, the ammonia concentration can be determined.

$$ppm = \left(\frac{1}{0.7860} * \frac{R_s}{8.19}\right)^{-0.539} \tag{4.5}$$

5

Design Concept

5.1. Concept

For the ammonia sensor, and MICS-5914 MEMS sensor will be used and the DHT22 sensor will be used to monitor the temperature and humidity. The MICS-5914 was chosen because it contains an claimed range of 1 ppb to 10,000 ppb. According to [3], ammonia concentration is in a range between 0.5-8mM which is 9-144 ppm however this is dissolved ammonia so ammonia in gas phase must be less due to not all ammonia evaporating

These two sensors will be placed inside a perforated plastic cover. The reason for the cover is to remove the factor of high airflow as it would influence the measurements for the ammonia sensor. However a completely closed system would also lead to condensation which can also damage the sensors, thus the cover is perforated in order to provide ventilation. As seen in Figure 5.2, a circuit is drawn of how the sensors are connected to the Arduino Uno board. Additionally an SD card module is installed on the Arduino for datalogging and an external battery is used so the device does not need to be connected to a computer during the experiment.

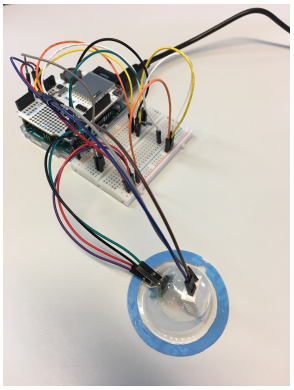

Figure 5.1: Concept of the sensor

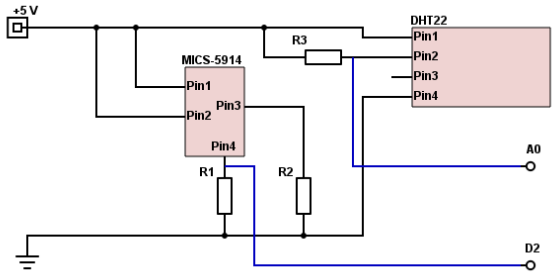

Figure 5.2: Circuit of the sensor to analog pin A0 and digital pin D2

5.2. Influencing Factors

Using a sensor which converts chemical signal into electrical signals has its limitations. The sensor needs some time in order to reach its chemical equilibrium. Direct airflow on the sensor surface will also change the conductivity of the sensor by altering the heated layer temperature. However these factors can easily removed by heating up the sensor before use. And as already mentioned in section 5.1, there is cup which prevents direct airflow from influencing the MICS-5914 sensor. However humidity and temperature are the 2 most important factors which influence the sensor.

5.2.1. Humidity

Environmental humidity is an important factor influencing the performance of metal oxide gas sensors, as many humidity gas sensors based on metal oxides have been developed. However, mechanism of sensing water vapor and other pollution gas such as CO, NO_2, H_2S, is different. For metal oxide humidity gas sensors, ionic-type humidity sensors are the most common patterns. The conduction mechanism depends on H^+ or H_3O^+ , from dissociation of adsorption water, which hops between adjacent hydroxyl groups. Water adsorbing on the metal oxide surface will not donate electrons to sensing layers. Moreover, as explained in [65] and [66], it will lower the sensitivity of metal oxide sensors for some reasons as follows. The reaction between the surface oxygen and the water molecules conduces to a decrease in baseline resistance of the gas sensor, and results in a decrease of the sensitivity [66]. Secondly, the adsorption of water molecules leads to less chemisorption of oxygen species on the SnO_2 surface due to the decrease of the surface area that is responsible for the sensor response [67]

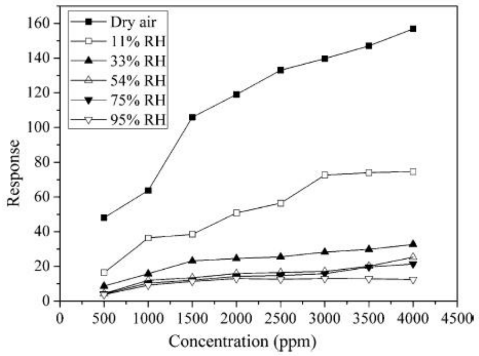

Figure 5.3: Response of the Sm_2O_3-doped SnO_2 sensor to different concentrations of C_2H_2 at different RH (adapted from [65])

5.2.2. Temperature

Temperature is also an important factor for the metal oxide gas sensors. Typical curves of gas response vs. temperature were shown in Figure 5.4. Gas sensors with different compositions have similar shapes. The responses increase and reach their maximums at a certain temperature, and then decreased rapidly with increasing the temperature. This tendency is commonly observed [67]. In reference [68], the authors considered that the shape resulted from the competition between slow kinetics at low temperatures and enhanced desorption at high temperatures.

- Use two ammonia sensor one covered to

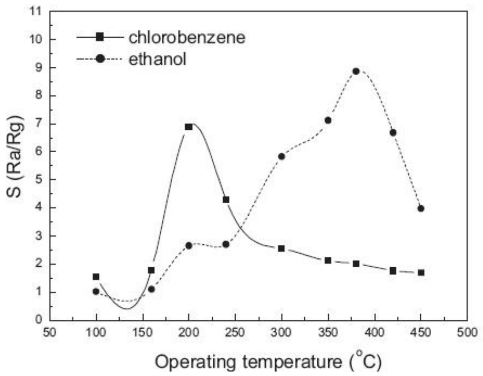

Figure 5.4: Gas response versus operating temperature of porous ZnO nanoplate sensor to 100 ppm chlorobenzene and ethanol (adapted from [69])

5.3. Preliminary Testing

Prior to conducting the experimental trial, the sensor was tested in vitro in a controlled environment. Six artificial sweat samples were created with distilled water and defined ammonia concentration ranging from 0.5 mM to 8 mM, which is the concentration range mentioned in chapter 3. An additional sample of distilled water was also used in order to see how the system reacts.

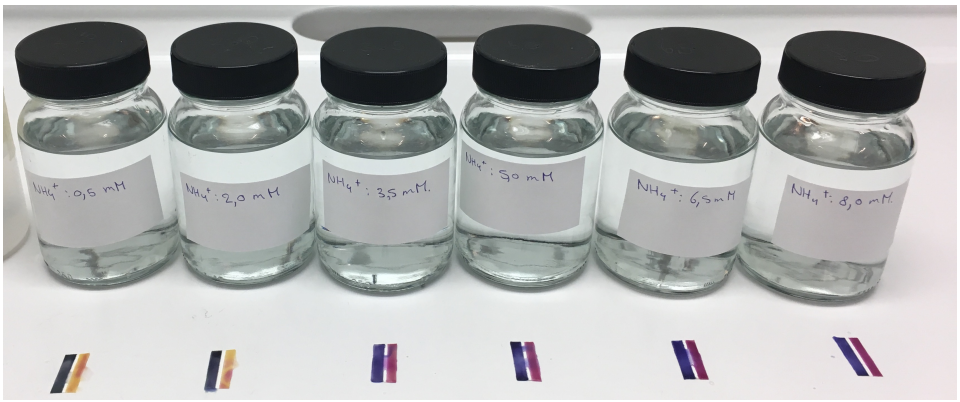

Figure 5.5: Five ammonia solution test samples ranging from 0.5mM - 8.0mM

For skin recreation a petri dish was placed on a hotplate with the temperature set at 30^{o}C which is approximately the average temperature of the upper leg [70]. One milliliter of each sample was used to monitor the sensor behavior at different concentrations.

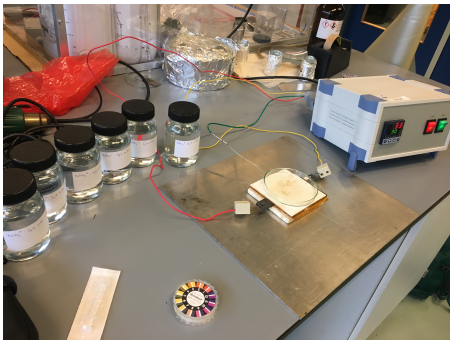

Figure 5.6: Test Setup

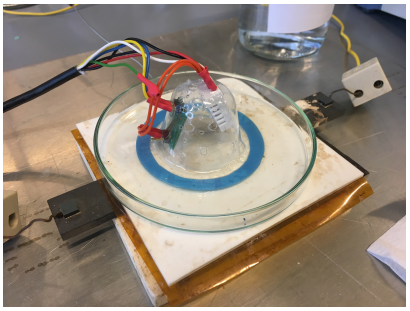

Figure 5.7: Sensor placed on the hot-plate

The result, which is shown in Figure 5.9 increase in voltage as result of a concentration increase. This is expect as the resistance of the MiCS 5914 sensor decrease, thereby increasing the voltage in the resistor, which is linked in series to the ammonia sensor.

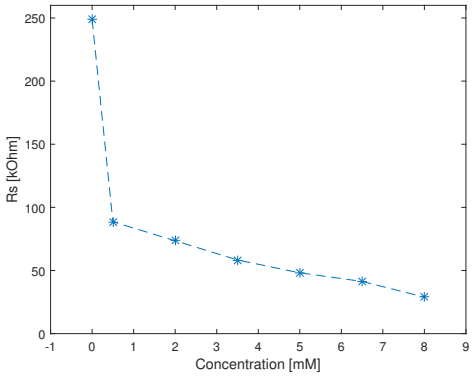

Figure 5.8: Voltage output at given ammonia concentrations

Using this data, it is possible to directly estimate the concentration of the ammonia solution in sweat without the need of determining the the ammonia concentration in gas phase as shown in subsection 4.2.5.

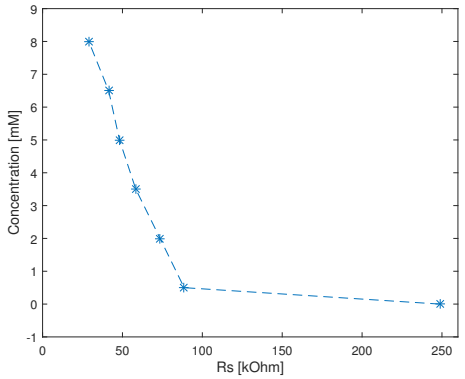

Figure 5.9: Estimated ammonia concentration in solution based on resistance of the sensor

For concentration greater than 0.5 mM, the sensor provides a linear trend as the resistance decreases. Concentrations between 0 an 0.5 mM does not seem to align with the remaining measurements. So for simplicity, two linear trends are used in order to determine the concentration.

If Rs is smaller than 90kOhm, for concentrations higher than 0.5mM ammonia solution, than the estimated ammonia solution concentration is:

$$c = -1.2956 * 10^{-4} * R_s + 11.5695 \tag{5.1}$$

And if Rs is greater than 90kOhm, for concentrations lower than 0.5mM ammonia solution, than the estimated ammonia solution concentration could be:

$$c = -3.1245 * 10^{-6} * R_s + 0.7769 \tag{5.2}$$

6

Experiment Method

6.1. Subject Selection and Sampling

One males (26) and one female (25) participated in this experiment. To participate in the experiment, the subjects had to: 1) initiate thermal sweating, 2) initiate sweating through exercise on an ergometer (*LODE Excalibur* ^{TM}) and 3) have no known metabolic conditions that may have adversely affected intermediary metabolism (e.g., diabetes, thyroid hormone disorder, hyperlipidemia). The subjects were informed of the nature of the trial, and all potential risks and benefits were explained to them.

6.2. Preparation & Setup

Before starting the experimental trial, it is advised that the participants are well-rested before conducting the experiment. Additionally, since the participants will exercise to the point of fatigue, the participants were also instructed not to eat a heavy meal 1-2 hours before the experiment.

The skin surface where the ammonia sensor concept is placed is cleaned with distilled water to remove possible contaminants.

The ammonia sensor is placed in close proximity to the muscle belly of the rectus femoris shown in Figure 6.1. Before the experimental trial, the ammonia sensor is placed and turned on 10 minutes prior to starting the experiment in order to warm up the embedded heater.

During the experiment, the participants breathes through a mask connected to a turbine flowmeter (*COSMED K5* ^{TM}) for continuous measurement of inspired and expired volume and by a mass spectrometer for continuous measurement of O_2 and CO_2 Figure 6.2.

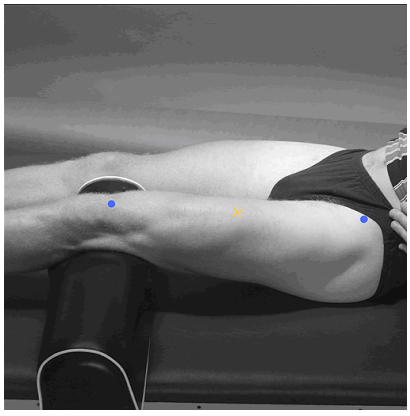

Figure 6.1: Sensor placement; on the yellow dot

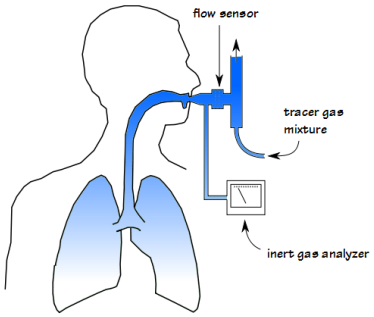

Figure 6.2: Respiratory gas analyser

6.3. Experimental trial

Two healthy participants (one males and one female) participated in the experiment. The sensor would then be placed on the left upperleg (Figure 6.1) for 10 minutes before the experimental trial.

The participants were to be seated on the *Excalibur sport* LODE bicycle ergometer with saddle height adjusted. The participant would start cycling at a power output of 80 Watt and a cadence of 80 RMP for 5 minutes. Afterwards, the participant continues cycling while the power output increases by 5 Watt every minute up to the point of fatigue. Afterwards the participants were continue cycling for 10 minutes at 80 W power output and 70 RMP cadence. If there is a increase in ammonia concentration during the incremental cycling exercise and a decrease during the resting period, this may imply that ammonia monitoring is a good constituent to indicate how fatigued the participant is on a scale from 0-100

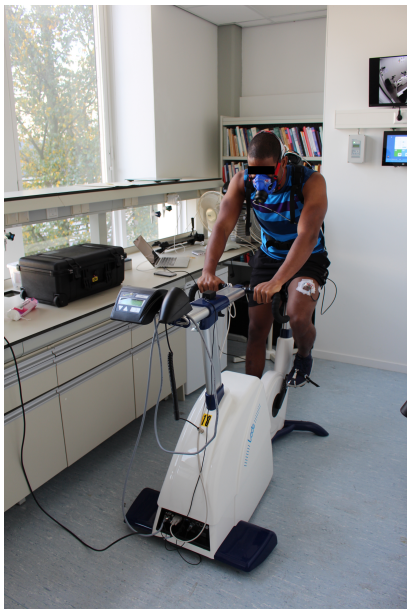

Figure 6.3: Experimental trial of participant 2

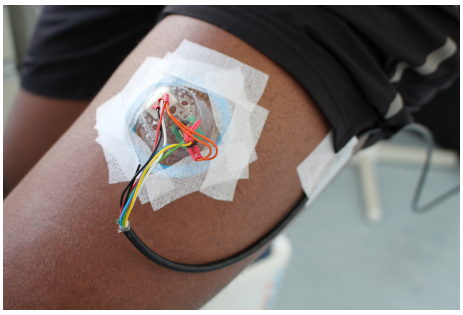

Figure 6.4: Sensor

6.4. Respiratory Exchange Ratio

A well documented method of defining when anaerobic metabolism occur is based on continuous measurement of respiratory gases and give a respiratory gases defined anaerobic threshold (RAT) [71]. The method for estimating RAT is by measuring the respiratory exchange ratio (RER), the relationship between expired CO_2 and inspired O_2. RER is calculated as follow:

$$RER = \frac{CO_2}{O_2} \tag{6.1}$$

The threshold is defined as an RER = 1.0 [72] [73]. Oxidation of fatty acid molecules occur when the RER is 0.7, whereas oxidation of carbohydrates occurs when the RER is 1.0. During resting period, RER ranges from 0.927 to 0.718 with an average of 0.817 ± 0.051 [74]. When RER higher than 1.0 indicates when anaerobic breakdown of glucose starts occurring. It is expected when fatigue starts to occur during the experimental trial, with some delay, a change in ammonia concentration is shown when RER is greater than 1.0

7

Results

The results of this experiment show little significant changes in ammonia concentration. Figure 7.3, Figure 7.6, Figure 7.2 and Figure 7.1 are divided in 4 sections within the experimental trial. As mentioned before, prior to start the experiment, there will be a 10 minute sensor warm up in which the participant remains still. The green vertical line indicates when the 5 minute warm up starts where both participants generated 80 Watt. The black vertical line indicates the start of the incremental cycling exercise starting at 85 Watt power output and increased by 5 Watt every minute. Participant 1 reached the point of fatigue at min 42:37 and participant 2 reached at min 46:25 the point of fatigue. These two points are indicated at the magenta vertical dotted lines.

7.1. Humidity

Prior to starting the experiment there is a noticeable decrease in humidity. It is highly probable that this is due to the distilled water which was used to clean the skin surface. Once the participants started cycling there is constant humidity level because the user is not sweating yet. When sweating occurs, the humidity starts to increase. The perforated holes in the design were intended to prevent the humidity from instantly reaching 100 RH%. However, if the sensor is placed on a a body section where no movement occurs (i.e. head and torso), despite the ventilation holes, the humidity would still reach 100 RH%. Because of the movement of the upper leg during cycling, as participants start sweating, the humidity gradually increases.

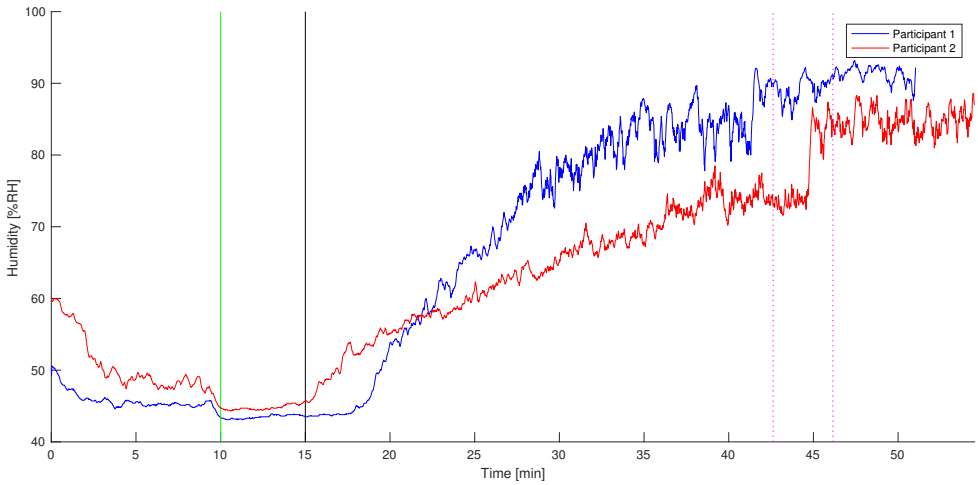

Figure 7.1: Humidity of both participants

	H [RH%] at minute 10	H [RH%] at minute 15	H [RH%] point of fatigue
Participant 1 (F)	43.4	43.5	89.8
Participant 2 (M)	44.7	45.7	85.0

Table 7.1

7.2. Temperature

The effect of the moving upperleg can also be seen in the temperature measurement. It would be expected that the temperature would increase during the exercise as the body temperature would rise. However, the same ventilation which prevents the humidity from increasing too quickly, also prevents the temperature from increasing. This is especially shown before the incremental exercise starts. The volume inside the cover starts to warm up through radiation of the body temperature. Once the participants starts cycling, the temperature decreases. Because the cadence was maintained at approximately 80 RPM, the temperature remained fairly constant as well.

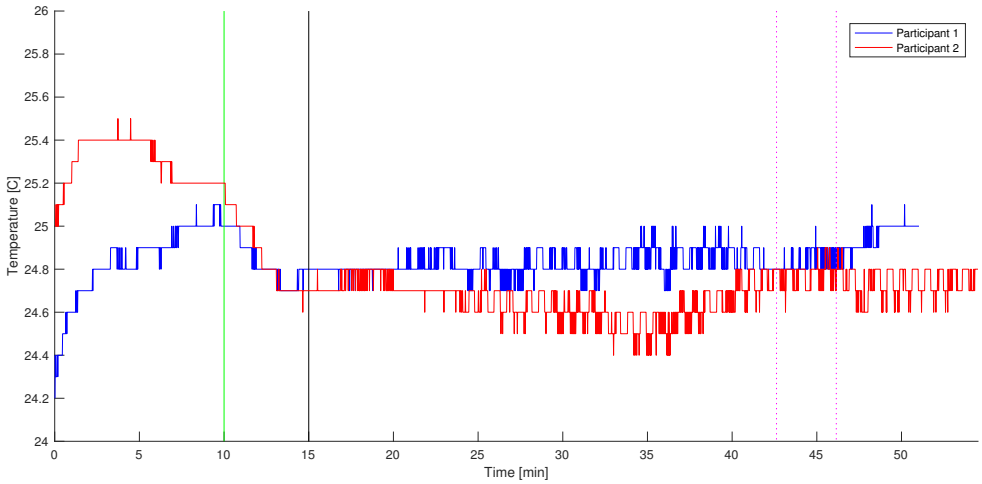

Figure 7.2: Temperature of both participants

	T [^{o}C] at minute 10	T [^{o}C] at minute 15	T [^{o}C] point of fatigue
Participant 1 (F)	25	24.80	24.80
Participant 2 (M)	25.2	24.70	24.80

Table 7.2

7.3. Ammonia concentration

7.3.1. Voltage output of the sensor

Similar to humidity, there is also an initial decrease in voltage output. However, this is most likely due to the sensor behaviour during the warm up Appendix F. After some time within 10 minutes, a value is reached in which no decrease occurs. In Figure 7.1 it is noticed for both participants that at the time when humidity starts to increase, the ammonia measurements start to increase as well. This was expected as the benefit of measuring ammonia in gas phase, as was previously mentioned in chapter 4, that measurements can be done prior to sweating occurring and can also be placed in locations where eccrine sweat glands produce less sweat.

Hence as humidity starts to increase and given that ammonia is able to evaporate more quickly than water due to its lower polarity, ammonia concentration can then be monitored. Though there is an

increase when humidity increases, there does not seem to be a dependency on the humidity. This can be seen as the ammonia not continuously increasing as humidity does. The correlation coefficient between ammonia concentration and the humidity is shown in Table 7.6.

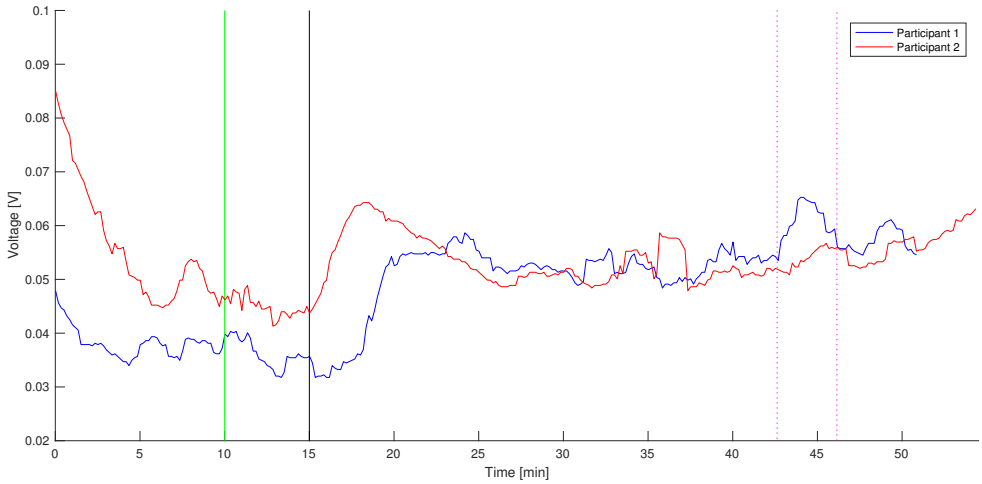

Figure 7.3: Ammonia concentration results of both participants

	Voltage at minute 10	Voltage at minute 15	Voltage at the point of fatigue
Participant 1 (F)	0.0347	0.0362	0.0538
Participant 2 (M)	0.0401	0.0425	0.0538

Table 7.3: Determined NH_3 concentrations at different times

7.3.2. Ammonia Solution in sweat

Determining the ammonia solution was done by using Equation 5.1 and Equation 5.2 based on the change in Rs.

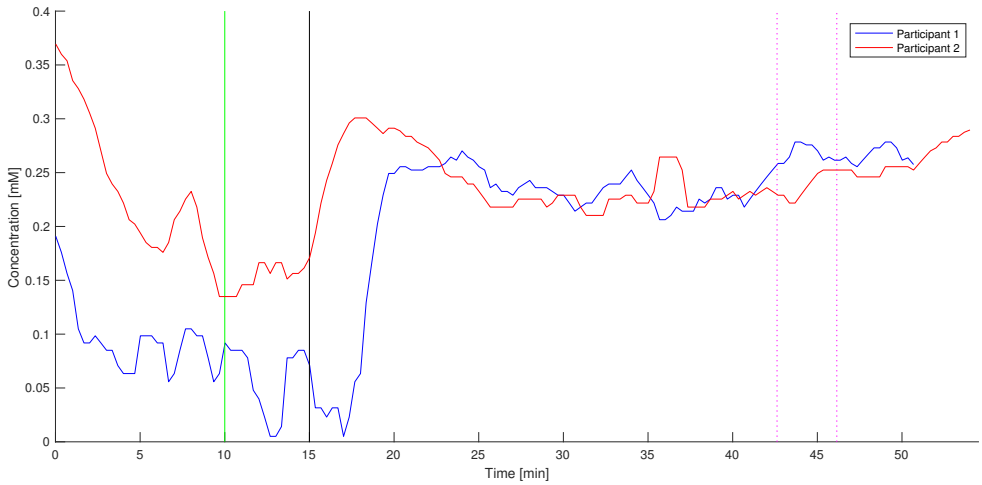

Figure 7.4: Ammonia concentration results of both participants

	NH_3 [mM] at minute 10	NH_3 [mM] at minute 15	NH_3 at the point of fatigue
Participant 1 (F)	0.0634	0.0850	0.2524
Participant 2 (M)	0.1349	0.1614	0.2524

Table 7.4: Determined NH_3 concentrations at different times

7.3.3. Ammonia gas concentration

When determining ammonia concentration in gas phase, the difference between participant 1 and 2 are different than in Figure 7.4 and Figure 7.3. The reason is that for both trials, the data output in the first ten minutes were used for re-calibration for both participant. The resistance (Rs) when only exposed to air was higher for participant 2 than participant 1. So this explains why the results for participant 2 is closer to the results of participant 1.

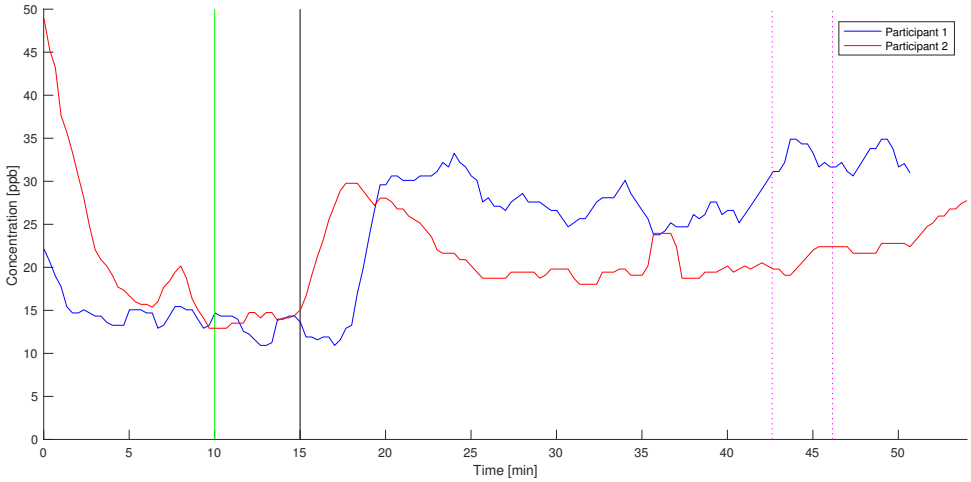

Figure 7.5: Ammonia gas concentration results of both participants

	NH_3 [ppb] at minute 10	NH_3 [ppb] at minute 15	NH_3 [ppb] at the point of fatigue
Participant 1 (F)	13.2669	14.3336	32.1901
Participant 2 (M)	12.9200	14.4328	22.3967

Table 7.5: Determined NH_3 concentrations at different times

Once the ammonia measurements starts increasing, the first 5-10 minutes, the behaviour is seems to differ between the two participants. After the rapid increase, the measurements of participant 2 relatively much more than participant. This can be due to multiple factor; gender, muscle mass, diet, genetics, amount of rest prior to starting the experiment.

After minute 25:00, there seems to be an similar ammonia trend up until the end of both trials. Both measurements gradually increases over time. However up to the point of fatigue at 42:37 (participant 1) and 46:25 (participant 2), there does not seem to be noticeable change in concentration which indicates fatigue.

7.4. Respiratory exchange Ratio

Similar to the ammonia measurements, measurements from the first 10 minutes must not be taken into consideration of the RER values. Inconsistent breathing pattern, due to talking and nervousness prior to starting cycling, is most probable cause for the high initial values and high fluctuations (for participant 2). As expected, the RER increases over during the trial. However, there is a sudden decrease for both participants. Initially, people will optimize their movement in order to minimize energy expenditure. This c

The correlation function is taken from There is no correlation between ammonia and the respiratory exchange ratio Figure 7.6 with an average correlation coefficient of $R^2 = -0.25$ (see Table 7.6).

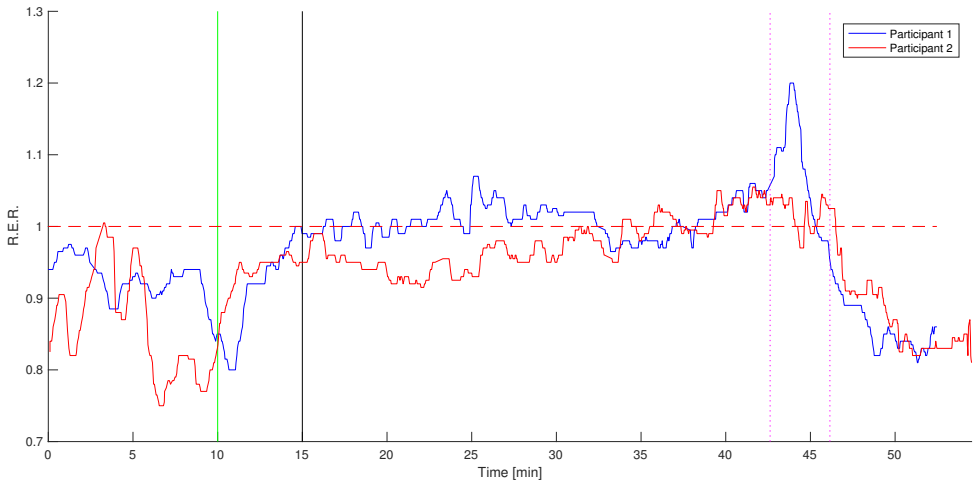

Figure 7.6: Respiratory exchange ratio of both participants: Above the horizontal line indicated anaerobic metabolism

The correlation were all taken after the 15 minute mark as this is the approximate time where some sweating starts to occur. It appears that there is low correlation between humidity, temperature and ammonia. However, the relatively higher correlation coefficients between temperature and humidity is due to the output values of humidity have some dependencies up to 8 RH% between the range of 10^{o}C and 40^{o}C [75]. Furthermore, there does not seem to appear anything noticeable from the correlation between these parameters.

	Ammonia (V)	Temperature	Humidity	R.E.R.
Ammonia (V)	1.0000	0.0409	0.0862	-0.2570
Temperature	0.0409	1.0000	-0.4751	-0.3960
Humidity	0.0862	-0.4751	1.0000	-0.2764
R.E.R.	-0.2570	-0.3960	-0.2764	1.0000

Table 7.6: Correlation coefficient average (R^2)

8

Discussion & Conclusion

In this work, the challenge was to design a non-invasive sensor to determine the state of muscle fatigue through sweat monitoring in real-time. In the first part of the paper, a number of sweat constituents were mentioned and under which conditions their concentration changes. Out of these constituents, ammonia seems to have the highest correlation with muscle fatigue. Afterwards, different methods where introduced of how these constituents can be monitored in real-time. Out of these methods, the MOS sensor was chosen. This is because there is an abundance in commercially available gas ammonia sensors which are often used in the automotive, chemical and industrial industries. Also the influence of sweat rate can be neglected.

8.1. Signal output

The results in Table 7.5 show an increase in ammonia concentration during incremental cycling activities. Ten minutes after the participants reached their point of fatigue, there is no noticeable decrease; although *Alvear* [25] does show a decrease after rugby training, measurement was done 24, 48 and 72 hours after rugby training. Thus it is possible that more time is needed in order to see a concentration decrease.

In the raw voltage output of the Arduino, a noticeable large amount of high peaks were present as seen in Figure 8.1. The many peaks which can be seen in the ammonia values have a high probability that is as result of an unstable voltage source. As an input source, a USB port of a *Macbook Pro (2013)* was used to power the Arduino. Currently, this problem was solved by applying a sliding window filter which divides the data up in a chosen window size of 10 seconds. In each window, the median was determined which removed the high values.

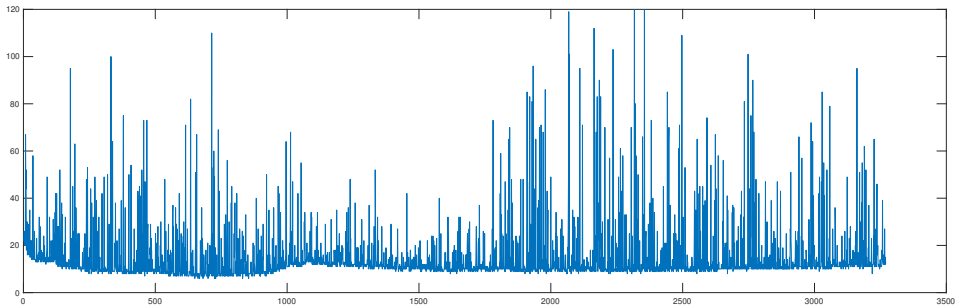

Figure 8.1: Raw voltage data of participant 2

8.2. Ammonia

In hindsight, the range of measurements of sweat ammonia is in question. Though the resulting ammonia concentrations are somewhat within the estimated range of 0.5-8 mM, the concentrations differences are much smaller than anticipated. Additionally, in this concept design, sweat can easily damage the MiCS 5914 sensor. The humidity can easily reach 99.9 RH% when perspiration occurs and as mentioned in subsection 5.2.1, it did not seem to influence the measurements itself. Salt which is also present in sweat, can corrode the circuit. Though there was no long exposure to high humidity, it appears that the sensor needed some re-calibration because there was an increase in resistance, most likely due to water adsorption. This can be resolved by re-calibrating the system every time the system is in use. This is also done by the Cosmed K5 respiratory sensor, which was used to determine the respiratory exchange ratio.

8.3. Humidity and Temperature

In order to keep the humidity low, larger holes were perforated in the plastic cover. Once sweating initiated during the experiment, the user must continue moving in order the push air out of the plastic cover and prevent humidity reaching 99.9 RH%. However, this may come at the cost of pushing out the ammonia before it could be monitored. For further researches, it is recommended to also monitor the airflow to and from the system.

Additionally, the necessary movement to keep the humidity low also explains the decrease in temperature as mentioned in chapter 7. However, temperature has very little influence on the sensor since there is a temperature change ΔT of 1^{o}C .

Long-time exposure to strong light and ultraviolet may decrease DHT22's performance. Occasional error in humidity measurements occur during long exposure to humidity. In several online forums, it was explained that the humidity calculation depends on the temperature values and can be reset by placing the sensor in an environment with a temperature ranging between 30-40^{o}C. For this experiment, this was not an issue, however if such device would be used in practice during a sporting activity, these factors also limit the reliability of the device.

8.4. Conclusion

Thus, the feasibility of determining muscular fatigue by non-invasively monitoring sweat ammonia concentrations is not yet definitive. Though there is a concentration increase, the values in which ammonia increases is questionable. Furthermore, there is no apparent decrease in ammonia at the end of the experiment, which may indicate that it takes longer to notice these changes when relaxed. However if this is the case, it may show that sweat analysis is too slow method for real time monitoring of muscle fatigue.

More research is required on this topic. For further research, it is adviced to use a MOS ammonia sensors with ranges in very low concentrations (<500 ppb). And in order to prevent the signal peaks, ensure a power supply is used that provides stable voltage. Additionally, a possibly better voltage output can by data-logged by connecting two ammonia sensor in a Wheatstone bridge circuit.

During the experiment it might be useful, prior to monitoring ammonia concentration during cycling task, to add an additional experiment to monitor ammonia concentrations during thermal sweating to test if ammonia concentration also changes when the participants sweat due to temperature. But most importantly, a larger number of data from multiple participants is required for a more concrete conclusion.

Note: *This paper is accepted for the 2019 Smart Systems Integration conference in Barcelona*

Bibliography

[1] D. G. Liebermann, L. Katz, M. D. Hughes, R. M. Bartlett, J. McClements, and I. M. Franks, *Advances in the application of information technology to sport performance,* Journal of sports sciences **20**, 755 (2002).

[2] Statistica, *Forecasted value of the global wearable devices market from 2012 to 2018 (in billion u.s. dollars),* https://www.statista.com/statistics/302482/wearable-device-market-value/, accessed: 2018-10-09.

[3] Z. Sonner, E. Wilder, J. Heikenfeld, G. Kasting, F. Beyette, D. Swaile, F. Sherman, J. Joyce, J. Hagen, N. Kelley-Loughnane, and R. Naik, *The microfluidics of the eccrine sweat gland, including biomarker partitioning, transport, and biosensing implications,* Biomicrofluidics **9**, 031301 (2015), https://doi.org/10.1063/1.4921039 .

[4] W. Gao, S. Emaminejad, H. Y. Y. Nyein, S. Challa, K. Chen, A. Peck, H. M. Fahad, H. Ota, H. Shiraki, D. Kiriya, *et al.*, *Fully integrated wearable sensor arrays for multiplexed in situ perspiration analysis,* Nature **529**, 509 (2016).

[5] M. Cifrek, V. Medved, S. Tonković, and S. Ostojić, *Surface emg based muscle fatigue evaluation in biomechanics,* Clinical Biomechanics **24**, 327 (2009).

[6] R. Merletti and D. Farina, *Myoelectric manifestations of muscle fatigue,* Wiley Encyclopedia of Biomedical Engineering (2006).

[7] B. K. Barry and R. M. Enoka, *The neurobiology of muscle fatigue: 15 years later,* Integrative and Comparative Biology **47**, 465 (2007), /oup/backfile/content$_public/journal/icb/47/4/10.1093/icb/icm047/2/icm047.pdf$.

[8] A. Guidi, A. Greco, F. Felici, A. Leo, E. Ricciardi, M. Bianchi, A. Bicchi, G. Valenza, and E. P. Scilingo, *Heart rate variability analysis during muscle fatigue due to prolonged isometric contraction,* in *Engineering in Medicine and Biology Society (EMBC), 2017 39th Annual International Conference of the IEEE* (IEEE, 2017) pp. 1324–1327.

[9] R. Merletti and P. A. Parker, *Electromyography: physiology, engineering, and non-invasive applications*, Vol. 11 (John Wiley & Sons, 2004).

[10] Y. Kuno, *Physiology of human perspiration* (J. And A. Churchill: London, 1934).

[11] D. Morris, S. Coyle, Y. Wu, K. T. Lau, G. Wallace, and D. Diamond, *Bio-sensing textile based patch with integrated optical detection system for sweat monitoring,* Sensors and Actuators B: Chemical **139**, 231 (2009), eUROPT(R)ODE IX Proceedings of the 9th European Conference on Optical Chemical Sensors and Biosensors.

[12] L. J, *Cyclic fluctuation of sweat electrolytes in women: Effect of polythiazide upon sweat electrolytes,* JAMA **195**, 629 (1966), /data/journals/jama/18818/jama$_1 95_{80} 18.pdf$.

[13] Z. Sonner, E. Wilder, J. Heikenfeld, G. Kasting, F. Beyette, D. Swaile, F. Sherman, J. Joyce, J. Hagen, N. Kelley-Loughnane, *et al.*, *The microfluidics of the eccrine sweat gland, including biomarker partitioning, transport, and biosensing implications,* Biomicrofluidics **9**, 031301 (2015).

[14] P. J. Derbyshire, H. Barr, F. Davis, and S. P. Higson, *Lactate in human sweat: a critical review of research to the present day,* The Journal of Physiological Sciences **62**, 429 (2012).

[15] I. Masui, *Changes of the electric resistance of the skin during sweating,* J. Jap. Physiol. Soc **7**, 448 (1942).

[16] W. Ladell, J. Waterlow, and M. F. Hudson, *Desert climate physiological and clinical observations,* The Lancet **244**, 491 (1944).

[17] W. Locke, N. B. Talbot, H. S. Jones, and J. Worcester, *Studies on the combined use of measurements of sweat electrolyte composition and rate of sweating as an index of adrenal cortical activity,* Journal of Clinical Investigation **30**, 325 (1951).

[18] D. B. Speedy, T. D. Noakes, and C. Schneider, *Exercise-associated hyponatremia: A review,* Emergency Medicine **13**, 17 (2001).

[19] S. Anastasova, B. Crewther, P. Bembnowicz, V. Curto, H. M. Ip, B. Rosa, and G.-Z. Yang, *A wearable multisensing patch for continuous sweat monitoring,* Biosensors and Bioelectronics **93**, 139 (2017).

[20] I. L. Schwartz and J. H. Thaysen, *Excretion of sodium and potassium in human sweat,* Journal of Clinical Investigation **35**, 114 (1956).

[21] G. Talbert and C. Haugen, *Simultaneous study of the constituents of the sweat, urine and blood, also gastric acidity and other manifestations resulting from sweating: I. chlorides,* American Journal of Physiology–Legacy Content **81**, 74 (1927).

[22] H. Spector, H. Mitchell, T. Hamilton, *et al.*, *The effect of environmental temperature and potassium iodide supplementation on the excretion of iodine by normal human subjects.* Journal of Biological Chemistry **161**, 137 (1945).

[23] H. Mitchell, T. Hamilton, W. Haines, *et al.*, *The dermal excretion under controlled environmental conditions of nitrogen and minerals in human subjects, with particular reference to calcium and iron.* Journal of Biological Chemistry **178**, 345 (1949).

[24] R. Green, R. Charlton, H. Seftel, T. Bothwell, F. Mayet, B. Adams, C. Finch, and M. Layrisse, *Body iron excretion in man: a collaborative study,* The American journal of medicine **45**, 336 (1968).

[25] I. Alvear-Ordenes, D. García-López, J. De Paz, and J. González-Gallego, *Sweat lactate, ammonia, and urea in rugby players,* International journal of sports medicine **26**, 632 (2005).

[26] D. Czarnowski, J. Gorski, J. Jóźwiuk, and A. Boroń-Kaczmarska, *Plasma ammonia is the principal source of ammonia in sweat,* European journal of applied physiology and occupational physiology **65**, 135 (1992).

[27] W. Ladell, *Creatinine losses in the sweat during work in hot humid environments,* The Journal of physiology **106**, 237 (1947).

[28] S. ITOH, I. FUJISHIRO, T. SUCHI, and K. SHIMOKATA, *The secretion of sugar and its intermediate substances in sweat and saliva,* The Japanese journal of physiology **3**, 10 (1952).

[29] M. S. Talary, F. Dewarrat, D. Huber, and A. Caduff, *In vivo life sign application of dielectric spectroscopy and non-invasive glucose monitoring,* Journal of Non-Crystalline Solids **353**, 4515 (2007).

[30] W. C. LOBITZ and A. E. OSTERBERG, *Chemistry of palmar sweat: Iii. reducing substances (glucose),* Archives of dermatology and syphilology **56**, 819 (1947).

[31] S. Wolfe, G. Cage, M. Epstein, L. Tice, H. Miller, and R. Gordon Jr, *Metabolic studies of isolated human eccrine sweat glands,* Journal of Clinical Investigation **49**, 1880 (1970).

[32] J. Green, P. Bishop, I. Muir, J. McLester Jr, and H. Heath, *Effects of high and low blood lactate concentrations on sweat lactate response,* International journal of sports medicine **21**, 556 (2000).

[33] M. J. Buono, N. V. Lee, and P. W. Miller, *The relationship between exercise intensity and the sweat lactate excretion rate,* The Journal of Physiological Sciences **60**, 103 (2010).

[34] W. Ament, J. Huizenga, G. Mook, C. Gips, and C. Verkerke, *Lactate and ammonia concentration in blood and sweat during incremental cycle ergometer exercise,* International journal of sports medicine **18**, 35 (1997).

[35] A. Whitehouse, *The dissolved constituents of human sweat,* Proceedings of the Royal Society of London. Series B, Biological Sciences **117**, 139 (1935).

[36] D. A. Sakharov, M. U. Shkurnikov, M. Y. Vagin, E. I. Yashina, A. A. Karyakin, and A. G. Tonevitsky, *Relationship between lactate concentrations in active muscle sweat and whole blood,* Bulletin of Experimental Biology and Medicine **150**, 83 (2010).

[37] S. P. Sinkeler, H. A. Daanen, R. A. Wevers, T. L. Oei, E. M. Joosten, and R. A. Binkhorst, *The relation between blood lactate and ammonia in ischemic handgrip exercise,* Muscle & Nerve: Official Journal of the American Association of Electrodiagnostic Medicine **8**, 523 (1985).

[38] D. Czarnowski and J. Gorski, *Sweat ammonia excretion during submaximal cycling exercise,* Journal of Applied Physiology **70**, 371 (1991).

[39] J. Lowenstein, *Ammonia production in muscle and other tissues: the purine nucleotide cycle.* Physiological Reviews **52**, 382 (1972).

[40] B. Mutch and E. Banister, *Ammonia metabolism in exercise and fatigue: a review.* Medicine and science in sports and exercise **15**, 41 (1983).

[41] B. Timmer, W. Olthuis, and A. Van Den Berg, *Ammonia sensors and their applications—a review,* Sensors and Actuators B: Chemical **107**, 666 (2005).

[42] S. W. Brusilow and E. H. Gordes, *Ammonia secretion in sweat,* American Journal of Physiology-Legacy Content **214**, 513 (1968).

[43] J. Huizenga, A. Tangerman, and C. Gips, *Determination of ammonia in biological fluids,* Annals of clinical biochemistry **31**, 529 (1994).

[44] T. Guinovart, A. J. Bandodkar, J. R. Windmiller, F. J. Andrade, and J. Wang, *A potentiometric tattoo sensor for monitoring ammonium in sweat,* Analyst **138**, 7031 (2013).

[45] A. Zoerner, S. Oertel, M. P. Jank, L. Frey, B. Langenstein, and T. Bertsch, *Human sweat analysis using a portable device based on a screen-printed electrolyte sensor,* Electroanalysis **30**, 665 (2018).

[46] H. Lee, C. Song, Y. S. Hong, M. S. Kim, H. R. Cho, T. Kang, K. Shin, S. H. Choi, T. Hyeon, and D.-H. Kim, *Wearable/disposable sweat-based glucose monitoring device with multistage transdermal drug delivery module,* Science Advances **3**, e1601314 (2017).

[47] P. K. Nagar, R. Maheshwari, and V. Pandey, *An approach of ion selective electrode for human body, cells and biomedical researches,* in *2016 International Conference on Micro-Electronics and Telecommunication Engineering (ICMETE)* (2016) pp. 499–503.

[48] D. Diamond, S. Coyle, S. Scarmagnani, and J. Hayes, *Wireless sensor networks and chemo-/biosensing,* Chemical reviews **108**, 652 (2008).

[49] D. S. Oertel, D. M. Jank, B. Schmitz, and D. N. Lang, *Monitoring of biomarkers in sweat with printed sensors combined with sport wearables,* in *Proceedings of the 2016 ACM International Joint Conference on Pervasive and Ubiquitous Computing: Adjunct* (ACM, 2016) pp. 893–898.

[50] S. Joshi, V. D. Bhatt, H. Wu, M. Becherer, and P. Lugli, *Flexible lactate and glucose sensors using electrolyte-gated carbon nanotube field effect transistor for non-invasive real-time monitoring,* IEEE Sensors Journal **17**, 4315 (2017).

[51] L. L. Tan, A. Musa, and Y. H. Lee, *Determination of ammonium ion using a reagentless amperometric biosensor based on immobilized alanine dehydrogenase,* Sensors **11**, 9344 (2011).

[52] T. Thorsen, I. Weaver, E. Holihan, R. Cabrera, and R. Sarpeshkar, *Flexible glucose sensors and fuel cells for bioelectronic implants,* in *2017 IEEE 60th International Midwest Symposium on Circuits and Systems (MWSCAS)* (2017) pp. 619–622.

[53] J. Park, C.-S. Kim, and M. Choi, *Oxidase-coupled amperometric glucose and lactate sensors with integrated electrochemical actuation system,* IEEE Transactions on Instrumentation and Measurement **55**, 1348 (2006).

[54] D. Morris, S. Coyle, Y. Wu, K. T. Lau, G. Wallace, and D. Diamond, *Bio-sensing textile based patch with integrated optical detection system for sweat monitoring,* Sensors and Actuators B: Chemical **139**, 231 (2009).

[55] C.-T. Wang and C.-C. Chiang, *The application of a u-shaped whispering-gallery mode-based optical fiber sensor for glucose measurement,* in *Advanced Materials for Science and Engineering (ICAMSE), International Conference on* (IEEE, 2016) pp. 573–576.

[56] B. Czarnik-Matusewicz, K. Murayama, R. Tsenkova, and Y. Ozaki, *Analysis of near-infrared spectra of complicated biological fluids by two-dimensional correlation spectroscopy: protein and fat concentration-dependent spectral changes of milk,* applied Spectroscopy **53**, 1582 (1999).

[57] J. Wang, M. G. Sowa, M. K. Ahmed, and H. H. Mantsch, *Photoacoustic near-infrared investigation of homo-polypeptides,* The Journal of Physical Chemistry **98**, 4748 (1994).

[58] H. Chung, M. A. Arnold, M. Rhiel, and D. W. Murhammer, *Simultaneous measurements of glucose, glutamine, ammonia, lactate, and glutamate in aqueous solutions by near-infrared spectroscopy,* Appl. Spectrosc. **50**, 270 (1996).

[59] J. Y. Chen, R. Matsunaga, K. Ishikawa, and H. Zhang, *Main inorganic component measurement of seawater using near-infrared spectroscopy,* Applied spectroscopy **57**, 1399 (2003).

[60] J. Alander, V. Bochko, B. Martinkauppi, S. Saranwong, and T. Mantere, *A review of optical nondestructive visual and near-infrared methods for food quality and safety, International Journal of Spectroscopy*, **2013** (2013).

[61] S. Šašić and Y. Ozaki, *Short-wave near-infrared spectroscopy of biological fluids. 1. quantitative analysis of fat, protein, and lactose in raw milk by partial least-squares regression and band assignment,* Analytical Chemistry **73**, 64 (2001).

[62] S. Naisbitt, K. Pratt, D. Williams, and I. Parkin, *A microstructural model of semiconducting gas sensor response: The effects of sintering temperature on the response of chromium titanate (cto) to carbon monoxide,* Sensors and Actuators B: Chemical **114**, 969 (2006).

[63] P. J. Peterson, A. Aujla, K. H. Grant, A. G. Brundle, M. R. Thompson, J. Vande Hey, and R. J. Leigh, *Practical use of metal oxide semiconductor gas sensors for measuring nitrogen dioxide and ozone in urban environments,* Sensors **17**, 1653 (2017).

[64] A. Stolk, H. Noordijk, H. den Hollander, M. van Zanten, W. K. RJ, and W. van Pul, *Het verloop van de ammoniakconcentratie over 2005-2014,* (2017).

[65] Q. Qi, T. Zhang, X. Zheng, H. Fan, L. Liu, R. Wang, and Y. Zeng, *Electrical response of sm2o3-doped sno2 to c2h2 and effect of humidity interference,* Sensors and Actuators B: Chemical **134**, 36 (2008).

[66] J. Gong, Q. Chen, M.-R. Lian, N.-C. Liu, R. G. Stevenson, and F. Adami, *Micromachined nanocrystalline silver doped sno2 h2s sensor,* Sensors and Actuators B: Chemical **114**, 32 (2006).

[67] C. Wang, L. Yin, L. Zhang, D. Xiang, and R. Gao, *Metal oxide gas sensors: sensitivity and influencing factors,* Sensors **10**, 2088 (2010).

[68] A. Kolmakov, D. Klenov, Y. Lilach, S. Stemmer, and M. Moskovits, *Enhanced gas sensing by individual sno2 nanowires and nanobelts functionalized with pd catalyst particles,* Nano letters **5**, 667 (2005).

[69] Z. Jing and J. Zhan, *Fabrication and gas-sensing properties of porous zno nanoplates,* Advanced Materials **20**, 4547 (2008).

[70] T. J. Kelechi, B. K. Haight, J. Herman, Y. Michel, T. Brothers, and B. Edlund, *Skin temperature and chronic venous insufficiency,* Journal of vascular nursing **21**, 98 (2003).

[71] G. Solberg, B. Robstad, O. H. Skjønsberg, and F. Borchsenius, *Respiratory gas exchange indices for estimating the anaerobic threshold,* Journal of sports science & medicine **4**, 29 (2005).

[72] K. Dickstein, S. Barvik, T. Aarsland, S. Snapinn, and J. Millerhagen, *Validation of a computerized technique for detection of the gas exchange anaerobic threshold in cardiac disease,* American Journal of Cardiology **66**, 1363 (1990).

[73] M. P. Yeh, R. M. Gardner, T. Adams, F. Yanowitz, and R. Crapo, *" anaerobic threshold": problems of determination and validation,* Journal of Applied Physiology **55**, 1178 (1983).

[74] J. H. Goedecke, A. S. C. Gibson, L. Grobler, M. Collins, T. D. Noakes, and E. V. Lambert, *Determinants of the variability in respiratory exchange ratio at rest and during exercise in trained athletes,* American Journal of Physiology-Endocrinology And Metabolism **279**, E1325 (2000).

[75] Kandrsmith.org, *Test and calibrate dht22 hygrometers,* (2017).

[76] Y. Kondoh, M. Kawase, and S. Ohmori, *D-lactate concentrations in blood, urine and sweat before and after exercise,* European journal of applied physiology and occupational physiology **65**, 88 (1992).

[77] R. M. HARDEN, *Calcium excretion in thermal sweat in thyrotoxicosis,* Journal of Endocrinology **28**, 153 (1964).

A

Concentration of sweat constituents

Chemical	Molecular weight	Concentration [mM]	Concentration [ppm]	Trend when exercising
Pyruvate	88.06	42.9 - 67.6*	0.38 - 0.60	Decrease [76]
Glucose	180.156	0.001 - 1	0.18 - 180.15	Decrease [4]
Lactate	90.08	5 - 60	450.40 - 5404.80	Decrease [25] [13] [76]
Sodium	22.9898	10 - 100	229.90 - 2298.98	Increase [13] [4]
Chloride	35.453	10 - 100	354.53 - 3545.30	Increase [13] [4]
Potassium	39.0983	4 - 24	156.39 - 938.36	Decrease [13] [4]
Calcium	18.039	0.35 - 1.125	14 - 45	Unknown [77]
Magnesium	24.305	8.23 - 1366*	0.2 - 33.2	Unknown [10]
Phosphorus	30.97	0 - 1.5	0 - 48	Unknown [10]
Sulfate	96.06	0.42 - 1.77	40 - 170	Unknown [10]
Iodine	126.9	0.055*	0.007	Unknown [10]
Copper	63.546	0.94*	0.06	Unknown [10]
Manganese	54.94	1.092*	0.06	Unknown [10]
Iron	55.845	1.074 - 35.81*	0.06 - 2	Unknown [10]
Ammonium	18.039	0.5 - 8	9.02 - 144.31	Increase [13]
Ammonia	17.031	1.8 - 4.2	30.66 - 71.53	Increase [13] [25] [44]
Urea	46.07	2 - 6	120.12 - 360.36	Increase [25]
Amino acids	X	X	11 - 102	Unknown [10]
Uric acids	X	X	0 - 12	Unknown [10]
Creatine	131.13	15.3 - 144.9*	2 - 19	Unknown [10]
Ethanol	17.031	2.5 - 22.5	115.18 - 1036.58	X

Table A.1: * μM

B

Graphs of past researches of ammonia

Alvear

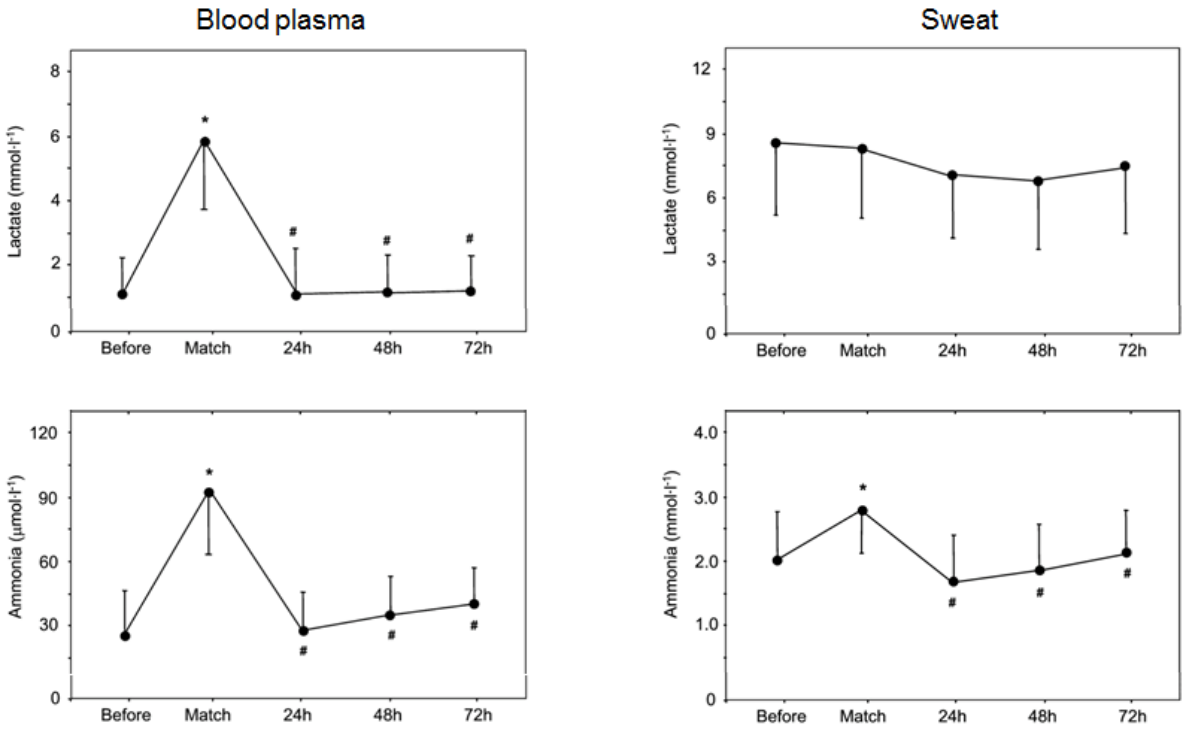

Figure B.1: Ammonia, lactate, and urea concentrations in blood in sweat. Samples were collected before rugby training, during the training, 24 hr, 48 hr and 72 hr after training

Guinovart

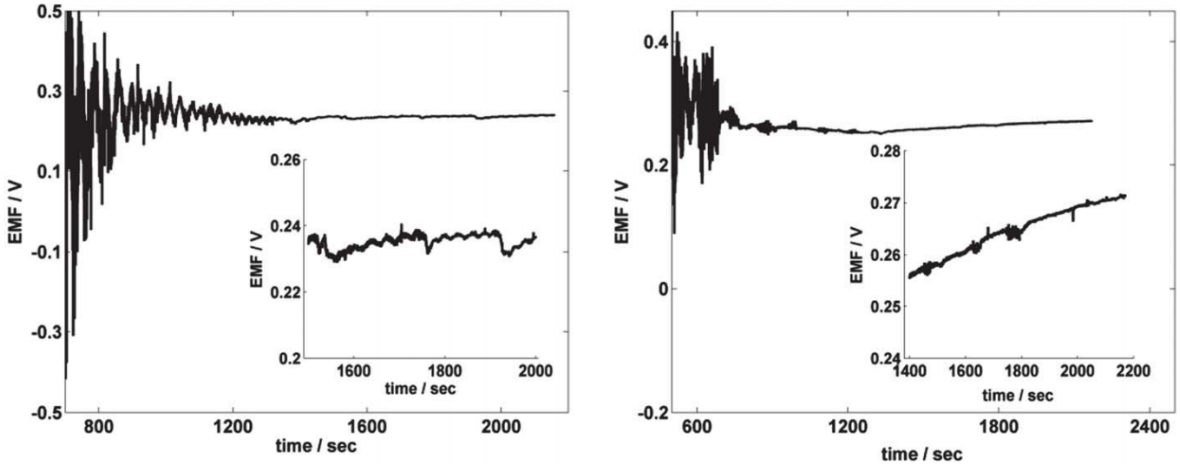

Figure B.2: Real-time data obtained from a human volunteer. The stable section corresponds to the onset of sweat of the volunteer. Left: subject only increasing the load. Right: subject sprinting every 5 minutes.

Zoerner

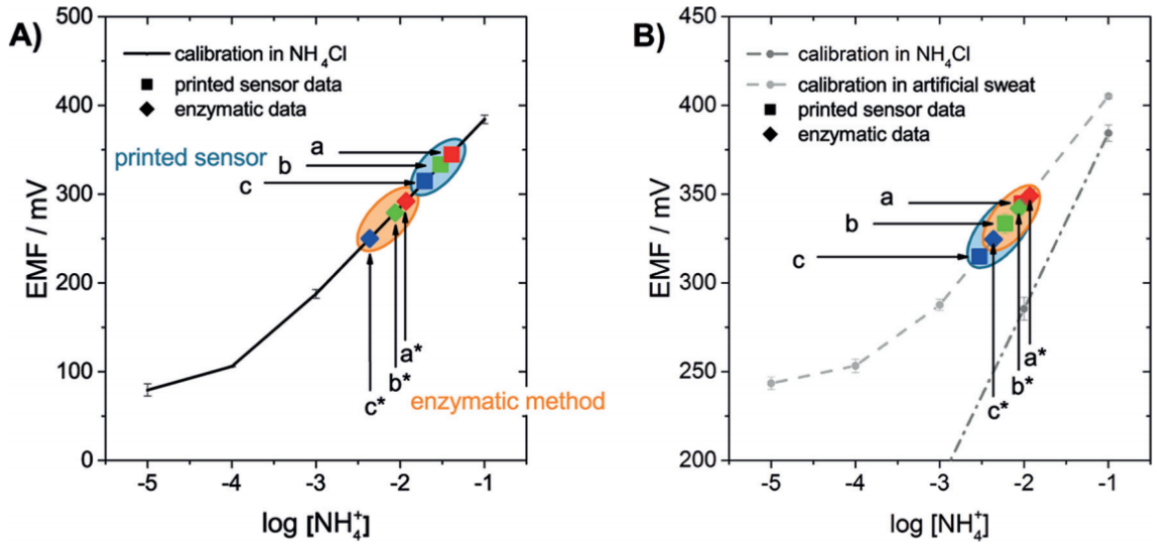

Figure B.3: A) Calculation of the ammonium concentration of real sweat samples for different loads of intensity (a) 240 W, b) 280 W and c) 320 W) using the calibration plot of ammonium chloride solutions. The resulting values of the enzymatic comparison measurement are also plotted for the different sweat samples of the intensity load (a*) 240 W, b*) 280 W, c*) 320 W). B) Calculation of the ammonium concentration using the calibration plot of artificial sweat measurement with different ammonium concentration for three different intensity levels

Ament

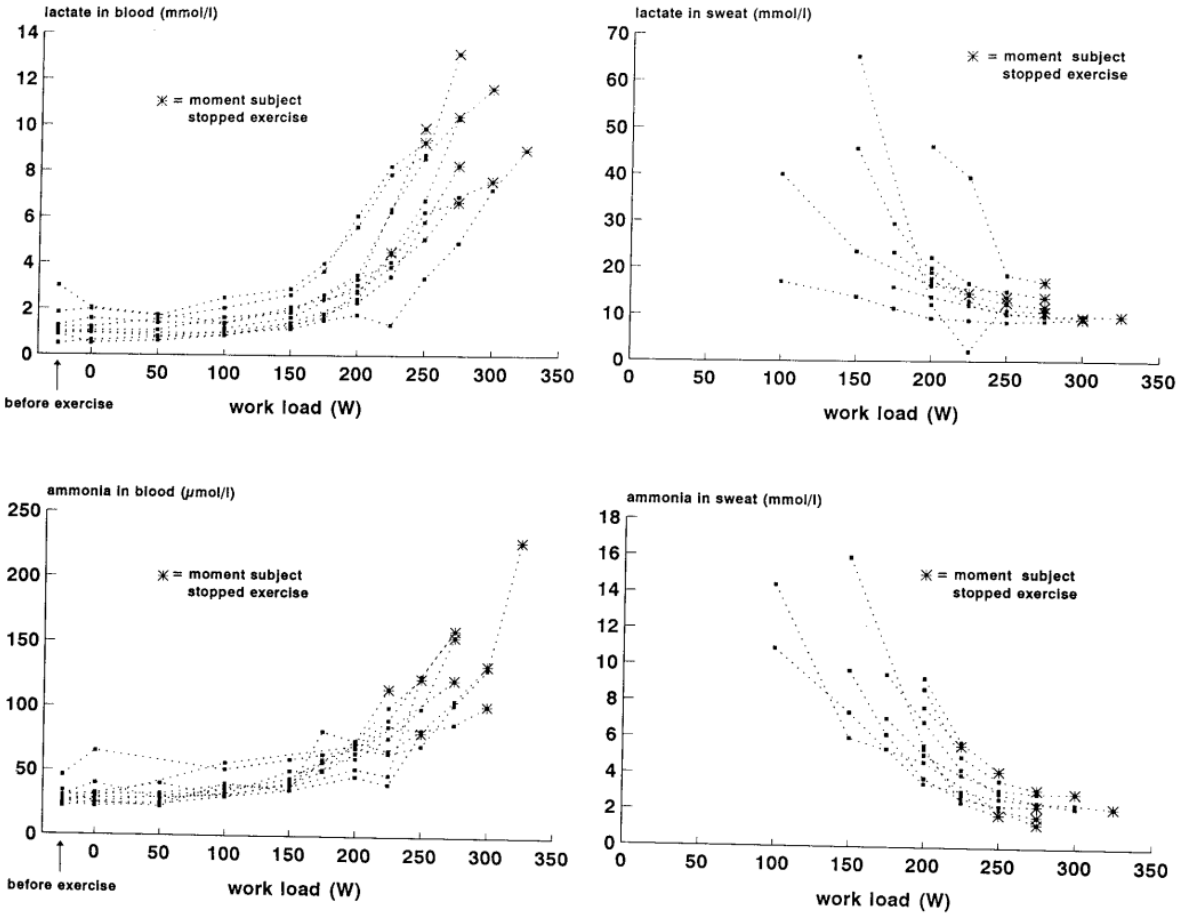

Figure B.4: Left: concentration of lactate (above) and ammonia (below) in blood of all subjects before and during incremental cycling exercise. Right: concentration of lactate (above) and ammonia (below) in sweat of all subjects before and during incremental cycling exercise

C

Arduino Code

```
#include <SPI.h>
#include <SD.h>
#include <dht.h>

#define dataPin 2 // Defines pin number to which the sensor is connected
dht DHT; // Creats a DHT object

#define DHT22_PIN 2

// Gas sensor reading
int Sensor = A0;

//SPI Settings
int pinCS = 10; // Pin 10 on Arduino Uno
int pow_pin = 8;
int LED_pin = 4;

void setup()
{
  Serial.begin(9600);
  Serial.println("Initializing Card");

  //CS Pin is an output
  pinMode(pinCS, OUTPUT);

  //LED on
  pinMode(LED_pin,HIGH);


  //Card will draw power from pin 8
  pinMode(pow_pin, OUTPUT);
  digitalWrite(pow_pin, HIGH);



  //Check if card is ready
  if (!SD.begin(pinCS))
  {
    Serial.println("Card Failed");
    return;
  }
  else
  {
    digitalWrite(LED_pin,HIGH);
    delay(1000);
    digitalWrite(LED_pin,LOW);

    delay(1000);
```

```
    digitalWrite(LED_pin,HIGH);
    delay(1000);
    digitalWrite(LED_pin,LOW);

    delay(1000);

    digitalWrite(LED_pin,HIGH);
    delay(1000);
    digitalWrite(LED_pin,LOW);

    delay(1000);


  }

  Serial.println("Card ready");
  Serial.println("Ammonia \tTemperature \tHumidity");

}

float Voltage;

void loop()
{
  int readData = DHT.read22(dataPin); // Reads the data from the sensor for DHT22 sensor
  int analogValue;                    // Reads the data from the sensor for MQ135 sensor

  float concentration;
  float t = DHT.temperature; // Gets the values of the temperature
  float h = DHT.humidity; // Gets the values of the humidity


  analogValue = analogRead(Sensor);
  Voltage = (float) analogValue; //(float) analogValue*5/2013;
  concentration = Voltage;



  // Write Data in Trial.TXT file
  File dataFile = SD.open("Trial.txt", FILE_WRITE);
  if (dataFile)
  {
    digitalWrite(LED_pin,HIGH);
    dataFile.print(concentration);
    dataFile.print(" ; "); dataFile.print(t); dataFile.print(" ; "); dataFile.println(h);
    dataFile.close();
    Serial.print(concentration); Serial.print("\t\t"); Serial.print(t); Serial.print("\t\t");
Serial.println(h);

  }
  else
  {
    Serial.println("Couldn't access file");

    digitalWrite(LED_pin,LOW);
  }


  delay(1000);


}
```

D

MATLAB Codes

```
clear all; clc; close all;

%% Data trend of SGX sensor
% Rs/Ro = a* (ppm) ^b
a = 0.786;   %
b = -0.539;  %

%% Calibration
% The goals is do determine Ro given the Rs & ppm in air is known;
tic

Rl = 3700;  % Load resistor [Ohm]
delay = (1/60)*(1000/1000); %Delay programmed in Arduino every 500[ms]

%% Sensor Concept Data Processing

D = importdata('VU_trial_Annemarijn.txt');%Acquire data from sensor

% DA = D(:,1);%smoothdata(D(:,1), filter, smooth_variable); % Ammonia sensor
DT = D(:,2);%smoothdata(D(:,2), filter, 1); % Temperature sensor
DH = D(:,3);%smoothdata(D(:,3), filter, 1); % Humidity sensor

% Median filtering of the Ammonia
DA_raw = D(:,1);

smooth_variable = 1; % If filtering is wanted increase value;
filter = 'movmedian';
Fs = 1;              % Frequency 2x a second
window = 10;          % Window size [s]
window_size = window*Fs;
step          = floor(length(DA_raw)/window_size);         % Amount of steps

DA2          = DA_raw(1:step*window*Fs);
Section        = reshape(DA2, window_size, step);

for i = 1:step
    DA_median(i)    =    median(Section(:,i));           % median frequency of each section
end

DA = smoothdata(DA_median, filter, smooth_variable);
x = delay*(1 : window_size : (window_size*step));

%%

x2 = delay*(1:length(DT));

for i  = 1:length(DA)
    V_out2(i)    = DA(i)*(5/1023);  % Value 0 - 1023 range at 5V
```

```
    Rs(i)       = Rl * ( 5 - V_out2(i)) / V_out2(i);

    % Ammonia solution [mM]
    if Rs(i) > 88620
        NH3_l2(i)    = ((Rs(i) - 248640)/-320041) + 1;
    else
%         NH3_l2(i)    = ((Rs2(i) - 89296)/-7718.2)  + 1;
NH3_l2(i)    = ((Rs(i) - 248640)/-320041) + 1;
    end

end

V_out = movmean(V_out2,10);
NH3_l = movmean(NH3_l2,10);

%% Respiratory Sensor Data Processing

R = importdata('Respirate_A.xls');      % Acquire data from gas sensor

% Synchronise time between the K5 and the MiCS5914 sensor
t_start = [-1  43]; % Time when R started in order to synchronise [min s]

smooth_variable2 = 20;
DR = smoothdata(R(:,4), filter, smooth_variable2);   % R.E.R. values

x_k5 = R(:, 25);

for k = 1: length(x_k5)
    x_synch(k) = x_k5(k) + t_start(1) + t_start(2)*(1/60);
end

%% Figure: Plot Graphs
figure(1)

Concentration_NH3 = NH3_l;


% Calculated NH3 concentration in solution
subplot(4,1,2)
plot(x,          Concentration_NH3, ...
    [10  10],     [max(Concentration_NH3) min(Concentration_NH3)],'g', ...
    [15  15],     [max(Concentration_NH3) min(Concentration_NH3)],'k',...
    [42.62  42.62],[max(Concentration_NH3) min(Concentration_NH3)],'r')
ylim([min(Concentration_NH3) max(Concentration_NH3)])
xlim([0  x2(end)])
ylabel('Concentration [mM]')
xlabel('Time [min]')

% Temperature
subplot(4,1,3)
plot(x2, DT,'-b', ...
    [10  10],     [max(DT) min(DT)],'g', ...
    [15  15],     [max(DT) min(DT)],'k',...
    [42.62  42.62],[max(DT) min(DT)],'r')
ylim([min(DT) max(DT)])
xlim([0  x2(end)])
ylabel('Temperature [C]')
xlabel('Time [min]')

% Humidity
subplot(4,1,4)
plot(x2, DH,'-b', ...
    [10  10],     [100 min(DH)],'g', ...
    [15  15],     [100 min(DH)],'k',...
    [42.62  42.62],[min(DH) 100],'r')
ylim([min(DH) 100])
xlim([0  x2(end)])
ylabel('Humidity [%RH]')
xlabel('Time [min]')
```

```
%% Figure 2: Plot Including Respiratory Exchange Ratio

% Voltage
figure(2)
subplot(3,1,1)
plot(x, V_out, ...
    [10 10],    [max(V_out) min(V_out)],'g', ...
    [15 15],    [max(V_out) min(V_out)],'k',...
    [42.62 42.62],[max(V_out) min(V_out)],'r')
% ylim([min(V_out)  max(V_out)])
xlim([0 x(end)])
xlabel('Time [min]')
ylabel('Voltage [V]')

% K5 RER
subplot(3,1,2)
hold on
plot(x_synch, DR, ...
    [10 10],    [0 2],'g', ...
    [15 15],    [0 2],'k',...
    [42.62 42.62],[0 2],'r')
plot(x_synch, ones(size(DR)),'--r')
xlim([0 x2(end)])
ylim([min(DR) 1.3])
xlabel('Time [min]')
ylabel('R.E.R.')

% Calculated NH3 concentration in solution
subplot(3,1,3)
plot(x,         Concentration_NH3, ...
    [10 10],    [100 -100],'g', ...
    [15 15],    [100 -100],'k',...
    [42.62 42.62],[100 -100],'r')
ylim([min(Concentration_NH3) max(Concentration_NH3)])
xlim([0 x(end)])
ylabel('Concentration [mM]')
xlabel('Time [min]')

%% Plot Power trend

xP = (1:round(x2(length(x2))));
P  = [0 0 0 0 0 0 0 0 0 ...
    80 80 80 80 80 85 90 95 100 105 110 115 120 125 130 135 140 ...
    145 150 155 160 165 170 175 180 185 190 195 200 205 210 215 ...
    220 0 0 0 0 0 0 0 0 0 0];

figure(1)
subplot(4,1,1)
stairs(P)
xlabel('Time[min]')
ylabel('Power [W]')
xlim([0 x2(end)])

toc
time = x2(end)

%% Correlation between Ammonia sensor and K5 Cosmed

len = linspace(1, length(V_out) , length(DR));
for z = 1:length(len)
    V(z) = V_out(round(len(z)));
end

corrcoef(V,DR)

%% Parameter difference between before and after exercise
DH_before = DH(10/delay);
DH_mid = DH(15/delay);
DH_after  = DH(round(42.62/delay));
Humidity = [DH_before, DH_mid, DH_after]
```

```
DT_before = DT(10/delay);
DT_mid = DT(15/delay);
DT_after  = DT(round(42.62/delay));
Temperature = [DT_before, DT_mid, DT_after]

V_before = V_out(round(10/(delay*window)));
V_mid = V_out(round(15/(delay*window)));
V_after  = V_out(round(42.62/(delay*window)));
Voltage = [V_before, V_mid, V_after]

NH3_before = NH3_l(round(10/(delay*window)));
NH3_mid = NH3_l(round(15/(delay*window)));
NH3_after  = NH3_l(round(42.62/(delay*window)));
Ammonia = [NH3_before, NH3_mid, NH3_after]
```

E

Experiment Results

In the following graphs, there is a green, black and red vertical line present. The definitions of these line are as follow:

1. Green = Start cycling warm-up at 80W power output
2. Black = Start incremental exercise until fatigue
3. Red = Point of fatigue

Participant 1

- Age : 25
- Gender : Female
- Height : 185 cm
- Weight : 57 kg

Figure E.1: Participant 1

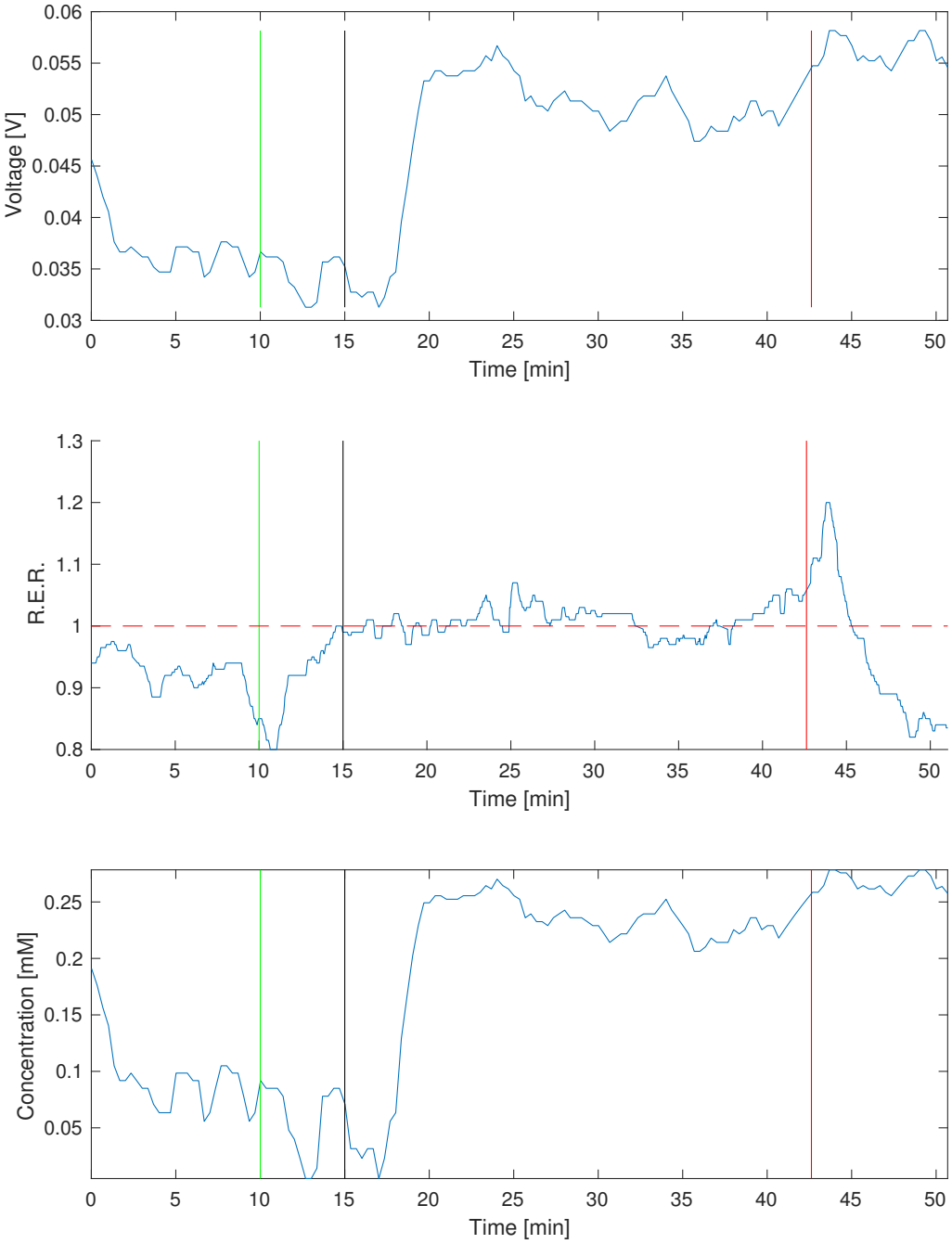

Figure E.2: Participant 1

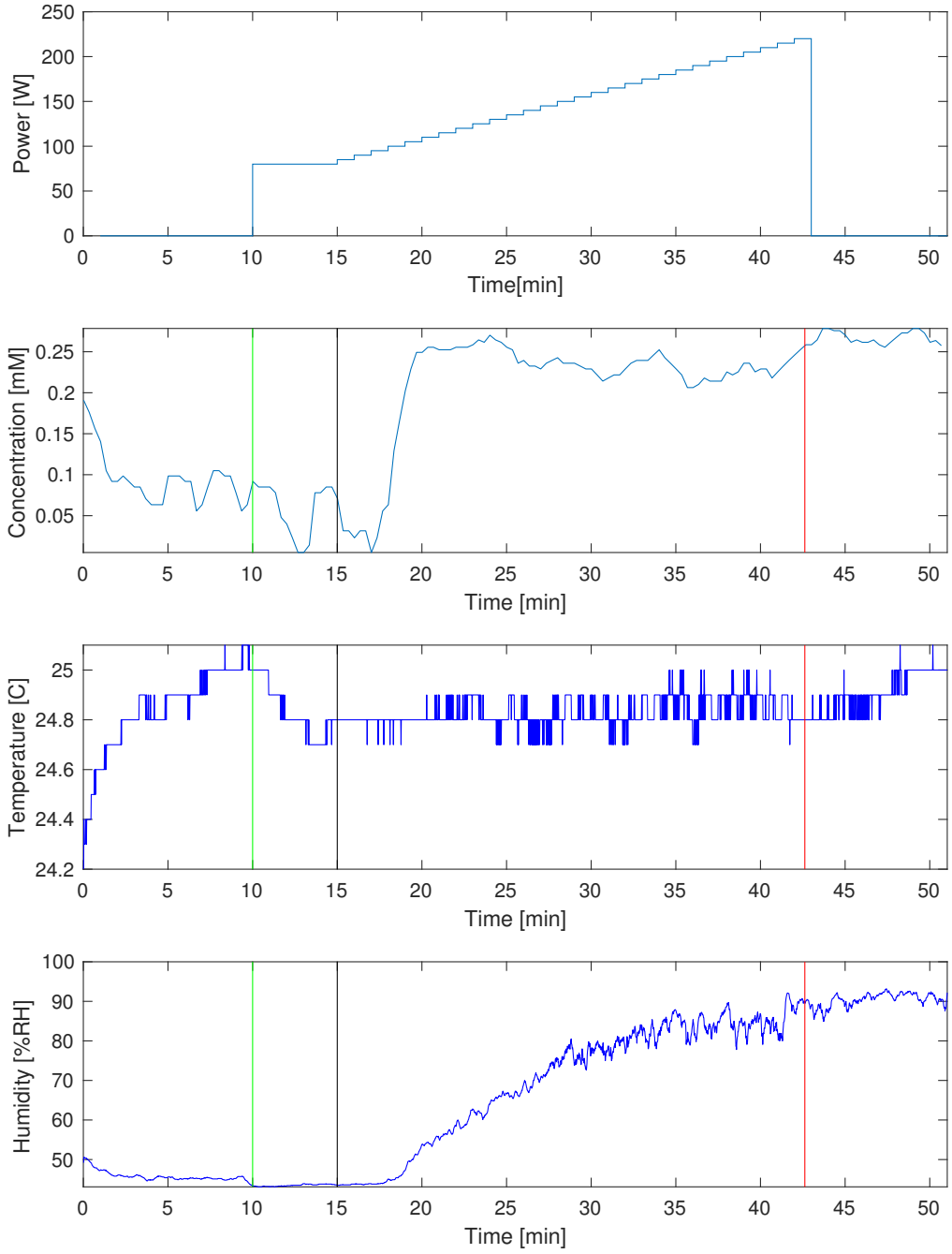

Participant 2

- Age : 26
- Gender : Male
- Height : 183 cm
- Weight : 93 kg

Figure E.3: Participant 2

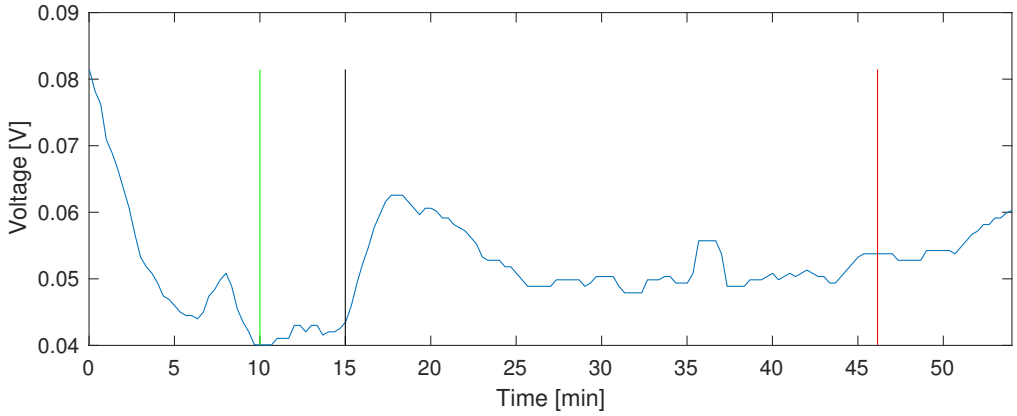

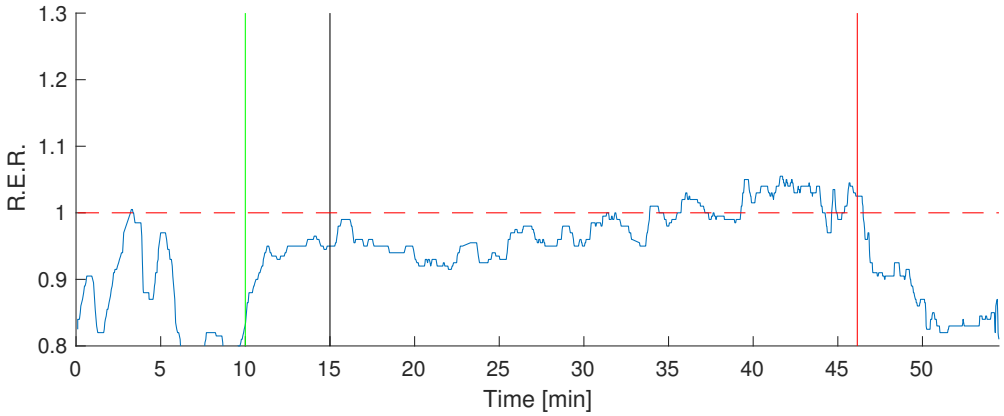

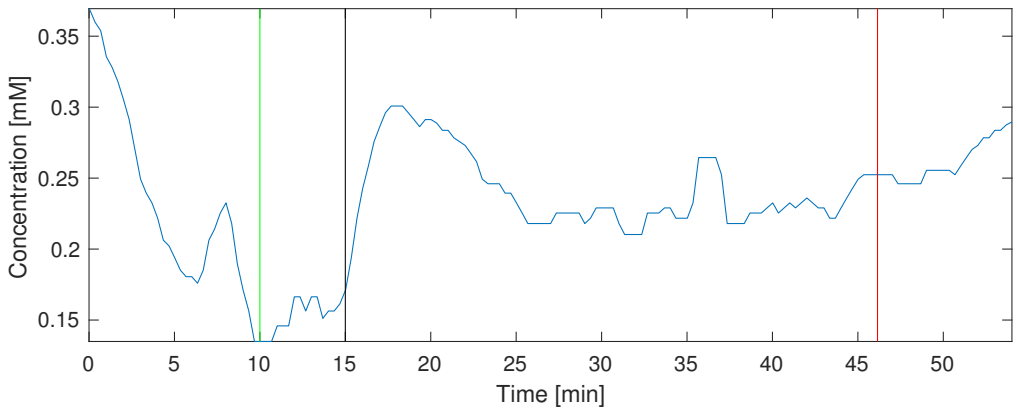

Figure E.4: Participant 2

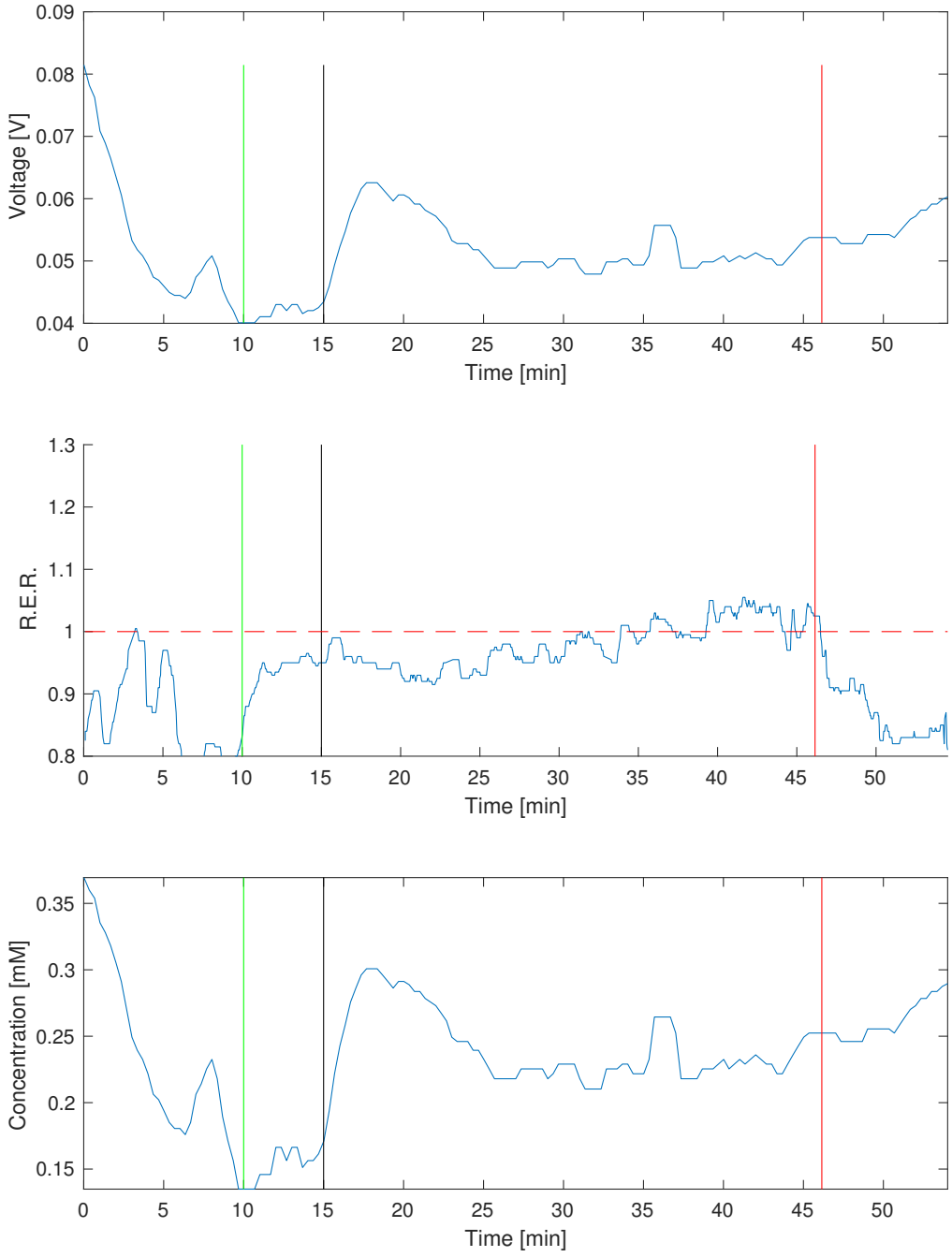

F

Sensor Behaviour

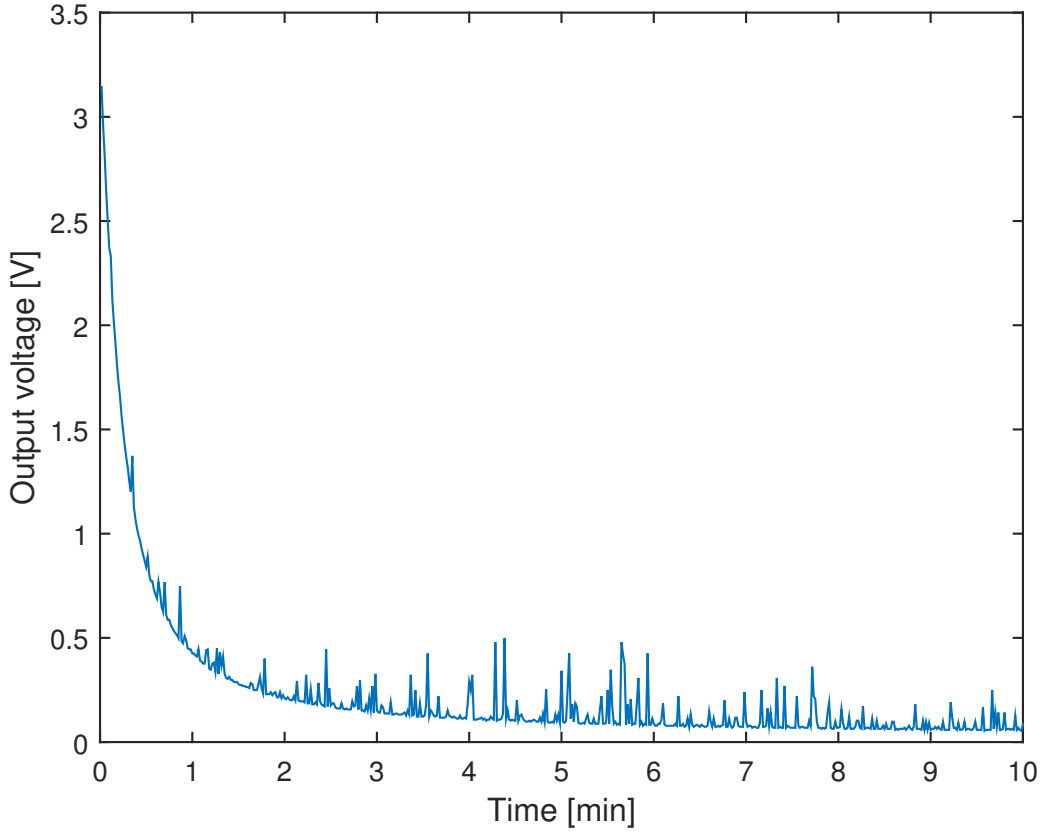

Figure F.1: Sensor behaviour in air during warm up when exposed to air